Nonlinear Dynamics and Systems Theory, **9** (4) (2009) 375–406

Analytical Methods for Analysis of Transitions to Chaotic Vibrations in Mechanical Systems

Yu.V. Mikhlin [1*], K.V. Avramov [2] and G.V. Rudnyeva [1]

[1] *Department of Applied Mathematics, National Technical University "KhPI", 21 Frunze St., Kharkov 61002, Ukraine*

[2] *Department of Nonstationary Vibrations, A.N. Podgorny Institute for Mechanical Engineering Problems, National Academy of Sciences of Ukraine, 2/10 Dm. Pozharskoho St., 61046, Kharkiv, Ukraine*

Received: March 27, 2008; Revised: September 3, 2009

Abstract: Some analytical methods for the analysis of transition to a chaotic behavior in nonlinear mechanical systems are considered here. First, the subharmonic Melnikov–Morozov theory, which is used to study a sequence of the saddle-node bifurcations, is considered. It is shown, that such bifurcations sequence occurs before an appearance of chaotic vibrations. Then, the chaotic dynamics in modulation equations is considered to study chaos in mechanical systems under the action of almost-periodic force, and the heteroclinic Melnikov functions are used to study the chaotic dynamics region. Finally, new approach for the construction of homo- and heteroclinic trajectories in some 2-DOF non-linear dynamical systems is used. Use of the Pade and quasi-Pade approximants, as well these approximants convergence condition make possible to solve boundary-value problems formulated for these orbits and to determine initial amplitude values of the trajectories with admissible precision.

Keywords: *chaotic vibrations; subharmonic bifurcations; homo- and heteroclinic trajectories.*

Mathematics Subject Classification (2000): 74H65, 70K44, 34C23.

* Corresponding author: muv@kpi.kharkov.ua

1 Introduction

Analysis of chaotic vibrations is a subject of intensive investigations during the last decades. One of the principal scenarios of the transient to chaotic behavior is a cascade of bifurcations of the period doubling. Two approaches exist to predict the chaotic behavior. Both these approaches hang one upon other. In the first approach, intersections of invariant manifolds, which lead to appearance of Smale horseshoe, are investigated to predict the chaotic dynamics. In the second approach, bifurcations of periodic and almost periodic vibrations are investigated to determine regions of the chaotic behavior. The subharmonic Melnikov–Morozov theory [1, 2 et al], which is considered in Section 2 of this paper, is related to the second approach. The methods, which are considered in Sections 3-6, are related to the first group of approaches. In particular, in Section 3 the Melnikov function is used to determine the region, where the heteroclinic structure exists in nonlinear mechanical systems under the action of almost-periodic excitation. Formation of homo- and heteroclinic trajectories (HT) in phase place is a criterion of the chaotic behavior in dynamical systems [1, 2 et al]. Methods, based on investigation of the HT formation, are related to the first group of approaches. (Note that the small dissipation leads to the complicated behavior near a separatrix of the Hamiltonian systems. Solutions that cross the separatrix due to the dissipation, were analyzed, for example, in [3]). The closed HT formation is possible in dynamical systems with dissipation and external periodic excitation. To construct the HT in such dynamical systems it is necessary to determine some important parameters. Namely, in such single-DOF system, it is necessary to know corresponding initial conditions of HT, and the functional dependence of the system parameters. For example, it may be a dependence of the external excitation amplitude on the dissipation parameter. In most cases the authors of the last and recent publications on HT construction make use of the well-known Melnikov function for the analysis of homoclinic structure [4-7], which gives a single equation for determination of unknown parameters. As a result, in the Melnikov condition, separatrix trajectories of the unperturbed autonomous equations are used. A problem of effective analytic approximation of HT of non-autonomous system is difficult and it is not solved up to now. Here a new approach for the HT construction in the nonlinear dynamical systems with phase space of dimensions equal to two is proposed and used. Pade approximants (PA) [8] and quasi-Pade approximants (QPA) are used to construct the HT in the dynamical system phase space and for the corresponding time history solution. Note that QPA which contain both powers of some parameter, and exponential functions were considered in Ref. [9]. Convergence condition were used earlier in the theory of non-linear normal vibration modes [10-12] as well as the conditions at infinity. This made possible to solve the boundary-value problem formulated for the HT and evaluate initial amplitude values with admissible precision. We suppose that the HT construction criterion of the chaos beginning proposed in this paper is more exact than the generally accepted Melnikov criterion, because it is not necessary to use separatrix trajectories of the Hamiltonian equations.

This work is structured as follows. First, the subharmonic Melnikov–Morozov theory and its application to parametric dynamics of beams are considered in Section 2. The method for determination of domains of chaos in mechanical systems under the action of quasiperiodic forces is considered in Section 3. The Pade approximants convergence condition is discussed in Section 4, and the HT boundary values problem is formulated in this Section. The approach proposed here was realized for the homoclinic solution of

the non-autonomous Duffing equation. Corresponding results are presented in Section 5. Construction of the homo- and heteroclinic orbits for the different dynamical systems is discussed in Section 6.

2 Subharmonic Melnikov–Morozov Theory and its Applications to Dynamics of Beam

Subharmonic Melnikov function analysis is carried out on the example of beam vibrations analysis. This beam is presented in Figure 2.1. Mass M is attached to the end of the beam. Transverse beam motions $W(s,t)$ induce displacements $\eta(t)$ of the mass M. Therefore, linear viscous damping force $R_L = c_L\dot{\eta}$ acts on the mass M. The nonlinear curvature and nonlinear inertia are taken into account in the model, so the equation of the beam parametric oscillations has the following form [13]:

$$\begin{aligned} EJw'''' + \tfrac{EJ}{2}\left(w''w'^2\right)'' + \left\{P_0 + P_t\cos(\bar{\Omega}t) - \tfrac{M}{2}\int\limits_0^l (w'^2)''_{tt}ds - \tfrac{c_L}{2}\int\limits_0^l (w'^2)'_t ds\right\} w'' \\ +c\dot{w} + \mu\ddot{w} - (Nw')' = 0, \\ N = \tfrac{\mu}{2}\int\limits_s^l ds_1 \int\limits_0^{s_1} (w'^2)''_{tt} ds_2, \end{aligned} \tag{2.1}$$

where $\dot{w} = w'_t; w' = w'_s$; μ is the mass per unit of length; $\dot{w}$ is the material damping; the term $w''''' + \frac{1}{2}(w''w'^2)''$ describes the beam curvature. The nonlinear inertia is presented by the term $(Nw')'$ in equation (2.1). The following dimensionless parameters are used:

$$\begin{aligned} &\varepsilon\delta = \frac{l^2}{\sqrt{EJ\mu}}; \varepsilon\delta_L = \frac{c_L w_*^2}{2l\sqrt{EJ\mu}}; \varepsilon\,\Gamma_t = \frac{l^2 P_t}{EJ}; \Gamma_0 = \frac{P_0 l^2}{EJ}; \varepsilon\,\gamma = \frac{w_*^2}{2l^2}; m = \frac{M}{\mu l}; \\ &u = \frac{w}{w_*}; \tau = \sqrt{\frac{EJ}{\mu l^4}}t;\ \xi = \frac{s}{l}; \Omega = \frac{\bar{\Omega} l^2\sqrt{\mu}}{\sqrt{EJ}};\ w_* = \frac{l2\sqrt{2}}{\pi}\sqrt{\frac{P_0}{P_*} - 1}, \end{aligned} \tag{2.2}$$

where $\varepsilon << 1; P_*$ is the buckling force; w_* is the static deflection at $s = \frac{l}{2}$. Equation (2.1) is rewritten in the dimensionless form:

$$\begin{aligned} &u''''' + \Gamma_0 u'' + \ddot{u} + \alpha(u''u'^2)'' + \varepsilon\left[-m\gamma\, u''\int\limits_0^1 \ddot{(u'^2)}d\xi - \gamma\left(u'\int\limits_\xi^1 d\eta\int\limits_0^\eta \ddot{(u'^2)}dh\right)' + \right. \\ &\left. +\delta\,\dot{u} + \Gamma_t os(\Omega\tau)u'' - \delta_L u''\int\limits_0^1 \dot{(u'^2)}d\xi\right] = 0, \end{aligned} \tag{2.3}$$

where $\alpha = 0.5\, w_*^2 l^{-2}$; $u' = u'_\xi; \dot{u} = u'_\tau$. Dimensionless fundamental frequencies of the corresponding linearized system (2.1) are the following: $p_k = k^2\pi^2$. The frequency Ω is varied in the next range: $0.5 < \Omega < 4$. Therefore, one mode approximation, $u = q(t)\sin(\pi\xi)$, accurately describes the beam dynamics. The following differential equation is derived by the Galerkin method:

$$\ddot{q} + \lambda(q^3 - q) + \varepsilon\left[\gamma\rho\pi^4 q(\dot{q}^2 + q\ddot{q}) + \delta\dot{q} - \Gamma_t\pi^2 q\cos(\Omega\tau) + \delta_L\pi^4\dot{q}q^2\right] + O(\varepsilon^2) = 0, \tag{2.4}$$

$$\lambda = \Gamma_0\pi^2 - \pi^4; \rho = m + \frac{1}{3} - \frac{3}{8\pi^2}. \tag{2.5}$$

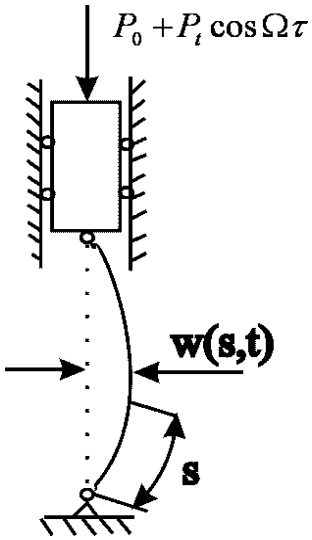

Figure 2.1: Transverse parametric oscillations of beam.

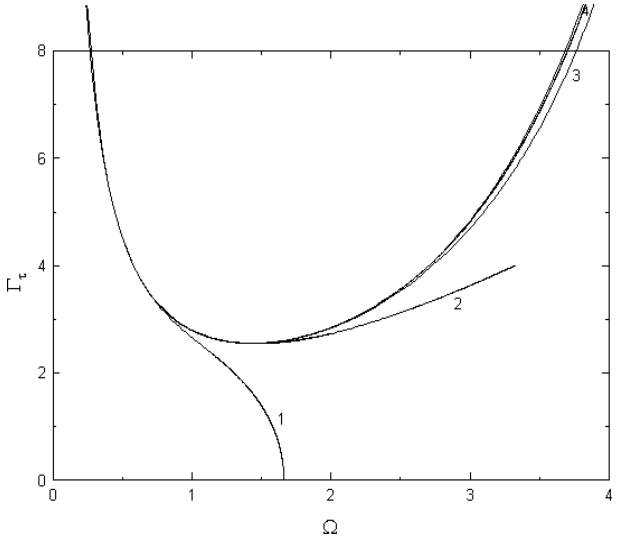

Figure 2.2: The saddle-node bifurcations curves of the subharmonic oscillations of orders 1,2,3,4. The curves are denoted by the same numbers. The calculations were performed with the following parameters: $\varepsilon = 0.01; \varepsilon\delta = \varepsilon\delta_L = 0.18; \varepsilon\gamma = 1.84 \cdot 10^{-3}; \rho = 3.4$.

The equation (2.4) can be presented as

$$\ddot{q} + \lambda(q^3 - q) + \varepsilon\left[-\gamma\rho\lambda\pi^4(q^5 - q^3) + \gamma\rho\pi^4 q\dot{q}^2 + \delta\,\dot{q} - \Gamma_t\pi^2 q\,\cos(\Omega\tau) + \delta_L\pi^4\dot{q}q^2\right] = 0. \tag{2.6}$$

We stress that, for $\varepsilon{=}0$ the system (2.6) is a nonlinear conservative one.

In the future calculations the beam dynamics is considered with the following parameters [14]:

$$E = 2.013\cdot 10^{11}\frac{N}{m^2};\ \rho = 7.80\cdot 10^3\frac{Kg}{m^3};\ l = 558mm; b = 11.95mm;\ h = 1mm;$$

$$M = 0.162Kg;\ \mu = 9.3\cdot 10^{-2}\frac{Kg}{m};\ P_* = 6.39N;\ P_0 = 6.42N; c = 7.8\cdot 10^{-2}\frac{Kg}{s};$$

$$EJ = 0.201Nm^2;\ w_* = 3.4\times 10^{-2}m.$$

Let us analyze the application of the Melnikov–Morozov method [1, 2, 4] for the saddle-node bifurcations analysis. It is known, that for $\varepsilon{=}0$ the system (2.6) allows the following periodic motions:

$$(q_0, \dot{q}_0) = \left\{\sqrt{\frac{2}{2-k^2}}dn\tau;\ -\frac{k^2\sqrt{2\lambda}}{2-k^2}sn\tau cn\tau\right\};\quad \tau = t\sqrt{\frac{\lambda}{2-k^2}}, \tag{2.7}$$

where k is the elliptic integral modulus; $dn; sn; cn$ are elliptic functions [15]. The equation: $H = \lambda(k^2-1)(2-k^2)^{-2}$ connects the Hamiltonian H of system (2.6) for $\varepsilon{=}0$ with the modulus of the elliptic integral. Let us consider motions of the system (2.6) meeting the resonance conditions:

$$T(k) = mT; T = {}^{2\pi}\!/_{\Omega}; T(k) = 2K\sqrt{{}^{2-k^2}\!/_{\lambda}}, \tag{2.8}$$

where K is the complete elliptic integral of the first kind; $T(k)$ is the period of the unperturbed system ($\varepsilon{=}0$) orbits. The subharmonic Melnikov–Morozov method permits to determine the subharmonic oscillations of a single DOF system with essential nonlinear unperturbed part. The simple roots of the subharmonic Melnikov function define these subharmonic oscillations. If the subharmonic Melnikov function roots meet the equation $|\sin(\Omega t_0)| = 1$, the saddle-node bifurcation set is taken place. The subharmonic Melnikov function of system (2.6) is derived as

$$\bar{M}_1^{m/1} = -\delta\sqrt{\lambda}J_1(k) + \Gamma_t\pi^2 J_3(k)\sin(\Omega t_0) - \delta_L\pi^4\sqrt{\lambda}J_2(k), \tag{2.9}$$

where

$$\begin{aligned}
J_1(k) &= \frac{1}{\sqrt{\lambda}}\int_0^{mT}\dot{q}_0^2 dt = \frac{4}{3}\left[(2-k^2)E - 2k'^2K\right](2-k^2)^{-3/2};\\
J_2(k) &= \frac{1}{\sqrt{\lambda}}\int_0^{mT}\dot{q}_0^2 q_0^2 dt = \frac{8}{15}\left[2(k^4+k'^2)E + (k^2-2)k'^2K\right](2-k^2)^{-5/2};\\
J_3\sin(\Omega t_0) &= \int_0^{mT} q_0\dot{q}_0\cos(\Omega\tau + \Omega t_0)d\tau = \frac{\Omega^2\pi}{\lambda sh\left(\frac{m\pi K'}{K}\right)}\sin(\Omega t_0).
\end{aligned} \tag{2.10}$$

Note that E is the complete elliptic integral of the second kind.

From the equation (2.9) the parametric set of saddle-node bifurcations is derived as

$$\Gamma_t = \pm\frac{\sqrt{\lambda}}{\pi^2 J_3(k)}\left[\delta_L \pi^4 J_2(k) + \delta J_1(k)\right]. \tag{2.11}$$

Figure 2.2 shows the saddle-node bifurcations curves on the parametric plane $(\Omega,\ \Gamma_t)$. The bifurcations curves of the subharmonic oscillations of orders 1,2,3,4 are denoted by the same numbers on this figure

$$(q_0, \dot{q}_0) = \left\{\sqrt{\frac{2k^2}{2k^2-1}}cn\tau; -\frac{k\sqrt{2\lambda}}{2k^2-1}sn\tau dn\tau;\right\}, \quad \tau = \frac{\sqrt{\lambda}t}{\sqrt{2k^2-1}}. \tag{2.12}$$

In this case, the equation $H = k^2 k'^2 \lambda (2k^2-1)^{-2}$ connects the Hamiltonian H with the elliptic integral modulus k. The subharmonic Melnikov function of these motions has the following form:

$$\bar{M}_1^{m/1} = -\delta\sqrt{\lambda}\hat{J}_1(k) + \Gamma_t \pi^2 \hat{J}_3(k)\sin(\Omega t_0) - \delta_L \pi^4 \sqrt{\lambda}\hat{J}_2(k), \tag{2.13}$$

$$\hat{J}_1(k) = \frac{8}{13}\left\{k'^2 K - (1-2k^2)E\right\}(2k^2-1)^{-3/2};$$

$$\hat{J}_2(k) = \frac{16}{15}\left\{Kk'^2(k^2-2) + 2E(k'^2+k^4)\right\}(2k^2-1)^{-5/2}; \quad \hat{J}_3(k) = \frac{2\Omega^2\pi}{\lambda sh\left(\frac{l\pi K'}{K}\right)}.$$

where $m = 2l; l = 1, 2, ...$ If $J_i (i = \overline{1,3})$ is replaced with $\hat{J}_i$ in formula (2.9), the equation of saddle-node bifurcations of the motions outside homoclinic orbit is obtained. Figure 2.3 shows the saddle-node bifurcations curves of subharmonic oscillations outside the homoclinic orbits of orders *m=2; m=4; m=6* for the system parameters from Section 1. The periodic motions of system (2.6) for *ε=0* outside the homoclinic orbit have the form:

Now the saddle-node bifurcations on the plane *(δ_L,Γ_t)* is considered. We study the limit cycles of the right homoclinic orbit on the system parametric plane. The equation (2.11) is rewritten as:

$$\Gamma_t = \pm\pi^2\sqrt{\lambda}J_2(k)J_3^{-1}(k)\left[\delta_L - \delta_L^*(m)\right], \tag{2.14}$$

where $\delta_L^*(m) = -\delta J_1(k)\pi^{-4}J_2^{-1}(k)$. Following [16], the values $\delta_L^*(m)$ are called the resonance numbers. Figure 2.4 shows qualitatively the bifurcations curves (2.14). As the elliptic integral modulus k satisfies the resonance condition (2.8), the following inequalities are true: $k(2.1) \prec k(2.2) \prec ... \prec k(\infty) = 1$. Note that the resonance numbers $\delta_L^*(m)$ satisfy the following relations: $\delta_L^*(\infty) = -1.25\delta\pi^{-4}$; $\lim\limits_{k\to 0}\delta_L^*(m) = -\delta\pi^{-4}$. From the analysis of the resonance numbers the following inequality is obtained: $\frac{d}{dk}\delta_L^*(k) < 0; k \in [k_1; 1]$. Therefore, integer number m_* can be selected, that the following inequalities are meet: $-1.25\delta\pi^{-4} = \delta_L^*(\infty) < ... < \delta_L^*(m_*+1) < \delta_L^*(m_*)$.

The intersections of the invariant manifolds of the saddle point are considered now. It is well known, that these intersections are the necessary condition for the existence of chaos [1, 2]. The homoclinic Melnikov function of beam has the following form:

$$M(t_0) = -\frac{4\sqrt{\lambda}\delta}{3} + \frac{\Gamma_t \pi^3 \Omega^2}{\lambda sh\left(\frac{\pi\Omega}{2\sqrt{\lambda}}\right)}\sin(\Omega t_0) - \frac{16}{15}\delta_L \pi^4\sqrt{\lambda}. \tag{2.15}$$

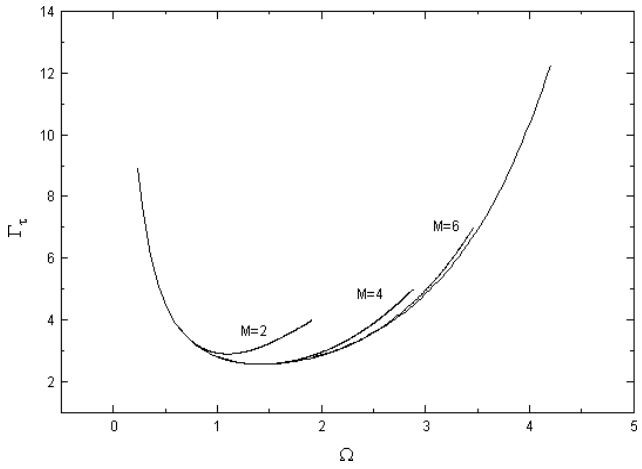

Figure 2.3: The saddle-node bifurcations curves of the subharmonic oscillations of orders m=2, m=4, m=6. The calculations are produced with the following parameters: $\varepsilon = 0.01; \varepsilon\delta = \varepsilon\delta_L = 0.18; \quad \varepsilon\gamma = 1.84 \cdot 10^{-3}; \rho = 3.4.$

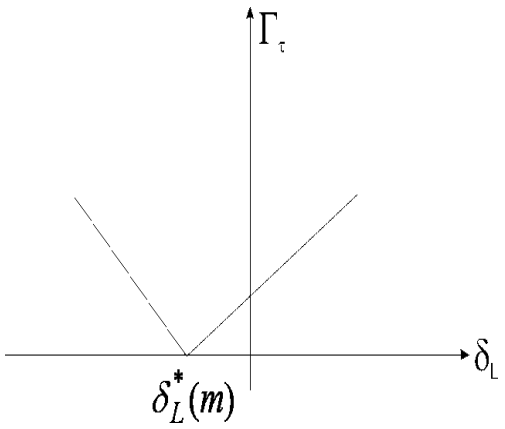

Figure 2.4: The qualitative behavior of the saddle-node bifurcation curve on the plane (δ_L,Γ_t).

The function M and subharmonic Melnikov function $\bar{M}_1^{m/1}$ satisfy the following limits:

$$\lim_{m\to\infty} \bar{M}_1^{m/1} = M\,. \tag{2.16}$$

Thus, the saddle-node bifurcations are obtained. However, the periodic motions, which undergo these bifurcations, are not studied. It is clear that these cycles may undergo others bifurcations. Here the Melnikov–Morozov method, which is considered in [4, 17], is used to study other bifurcations of parametric oscillations of beams.

The system (2.6) with respect to the action-angle coordinates *(I,θ)* can be written in the next form [17]:

$$\dot{I} = \varepsilon F(I,\theta,t); \dot{\theta} = \Omega_\Sigma(I) + \varepsilon G(I,\theta,t), \tag{2.17}$$

where $\Omega_\sum(I)$ is the frequency of the system (2.6) for ε=*0*. Let us consider the following motions:

$$I = I^{m,1} + \sqrt{\varepsilon}h(t); \theta = \Omega_\Sigma(I^{m,1})t + \phi, \tag{2.18}$$

where the values $I^{m,1}$ are obtained from the resonance conditions (2.8). Following [17], the oscillations $I = I^{m,1} + \sqrt{\varepsilon}h(t)$ are called the motions close to the resonance energetic level. The aim of the present study is an analysis of the topology of the Poincare sections close to the resonance energetic levels. Then the equations of the motions have the following form [1, 2]:

$$\dot{\bar{h}} = \frac{\sqrt{\varepsilon}}{2\pi}\bar{M}_1^{m/1}\left(\frac{\bar{\phi}}{\Omega_\Sigma(I^{m,1})}\right) + \varepsilon\bar{F}_I'\bar{h};\;\; \dot{\bar{\phi}} = \sqrt{\varepsilon}\frac{\partial\Omega(I^{m,1})}{\partial I}\bar{h} + \varepsilon\left[\frac{\Omega''(I^{m,1})}{2}\bar{h}^2 + \bar{G}(\bar{\phi})\right]. \tag{2.19}$$

The system (2.19) can be rewritten in the following form:

$$\begin{aligned}
&\dot{h} = \frac{1}{2\pi}\left(-\Delta_1\pi^4\sqrt{\lambda}J_2 + \Gamma_t\pi^2 J_3\sin m\phi\right) + \varepsilon h\left[\chi(\Delta_1) + \Gamma_t\pi^2 K_3\sin m\phi\right];\\
&\dot{\phi} = \Omega_\Sigma' h + \sqrt{\varepsilon}\left[\frac{\Omega_\Sigma''}{2}h^2 - \frac{\Gamma_t\pi^2 K_3}{m}\cos m\phi\right],
\end{aligned} \tag{2.20}$$

where $\Delta_1 = \delta_L - \delta_L^*; \chi = \delta\sqrt{\lambda}\dfrac{\Omega(2-k^2)^2\sigma(k)}{60\pi m\lambda k^3 J_2} - \Delta_1\pi^4\sqrt{\lambda}K_2;$

$$\sigma(k) = 80(2-k^2)E^2(k) - 160k'^2K(k)E(k) - 32(k^4+k'^2)K(k)E(k) + 16k'^2(2-k^2)K^2(k);$$

$$K_3 = \frac{\Omega\pi}{\lambda sh\left(\frac{m\pi K'}{K}\right)}\left[\frac{(2-k^2)^3\Omega^2\pi}{8\lambda k^4K^2k'^2}cth\left(\frac{m\pi K'}{K}\right) + \omega(k)\right];$$

$$K_2 = \frac{2E\Omega}{\lambda\pi m\sqrt{2-k^2}} + \frac{\omega(k)}{\Omega}J_2; \Omega_\Sigma' = -\frac{\sqrt{\lambda}\pi^2(2-k^2)[(2-k^2)E - 2k'^2K]}{2K^3k'^2k^4};$$

$$\Omega_\Sigma'' = -\frac{\sqrt{\lambda}\pi^3\left(2-k^2\right)^{5/2}}{4k^8k'^4}\left[\frac{2E(k'^6+3k'^2+k^4)}{K^4} + \frac{k'^2}{K^3}(4k'^2-k^4) - \frac{3E^2}{K^5}(2-k^2)^2\right].$$

The fixed points of the system (20) are the following:

$$(\phi_\nu, h_\nu) = \left(\frac{(-1)^\nu}{m}\arcsin(a) + \frac{\pi\nu}{m}; 0\right) + O(\varepsilon); \nu\in Z, \quad a = \frac{\sqrt{\lambda}}{\Gamma_t\pi^2 J_3}(\delta J_1 + \delta_L\pi^4 J_2). \tag{2.21}$$

If $a > 0 (a < 0)$, then ν is changed as: $\nu = 0, ..., 2m-1 (\nu = 1, ..., 2m)$.

Let us study these fixed points stability. System (20) is linearized and the eigenvalues λ of the constant matrix of the linear system are derived. The values λ of the saddle fixed points are the following:

$$\lambda_{1,2}^{(A)} = \pm\sqrt{\frac{\varepsilon}{2}\left|\Omega_{\Sigma}'\right|\Gamma_t \pi J_3 m\sqrt{1-a^2}} + O(\varepsilon). \tag{2.22}$$

The other group of the fixed points is denoted by B. The values λ of these fixed points are the following:

$$\lambda_{1,2}^{(B)} = \frac{1}{2}tr(\tilde{A}) \pm i\sqrt{\frac{\varepsilon}{2}\left|\Omega_{\Sigma}'\right|\Gamma_t \pi J_3 m\sqrt{1-a^2}}, \tag{2.23}$$

where $tr(\tilde{A})$ is the trace of matrix $[\tilde{A}]$, which meets the following limit:

$$\lim_{k\to 1} tr(\tilde{A}) = \lim_{k\to 1} \varepsilon\frac{\sqrt{\lambda}(\delta_L \pi^4 J_2 + \delta J_1)}{2mTk'^2 K(k)}. \tag{2.24}$$

Motions close to the resonance energetic levels have values k near 1. Using (2.24) we conclude that if

$$\delta_L < \delta_L^*(m) (\delta_L > \delta_L^*(m)), \tag{2.25}$$

the fixed points B are stable (unstable), respectively. From the inequality (2.25) the following parameter is introduced:

$$\alpha(k) = \delta\sqrt{\lambda}\frac{\Omega(2-k^2)^2\sigma(k)}{60\pi\, m\, \lambda\, k^3 J_2} + \Delta_1 \pi^4\sqrt{\lambda}\left(2K_3\frac{J_2}{J_3} - K_2\right).$$

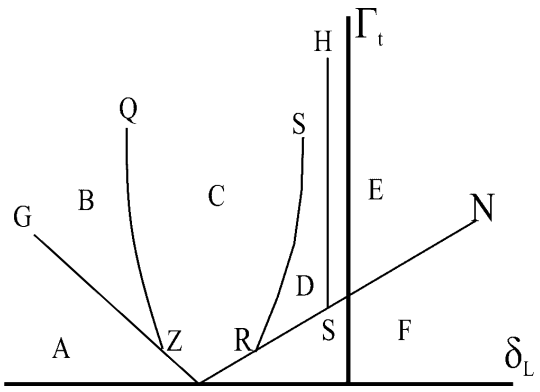

Figure 2.5: The curves of the saddle-node bifurcations and the heteroclinic bifurcations are shown. (QZ) and (RS) are the heteroclinic bifurcations curves. The letters denote the regions of the different dynamical behavior.

Then the inequality (2.25) can be rewritten as $\alpha < 0$ *(*$\alpha > 0$*).* Therefore, if $\alpha < 0$ *(*$\alpha > 0$), the fixed point B is stable (unstable), respectively. Therefore, the bifurcation set

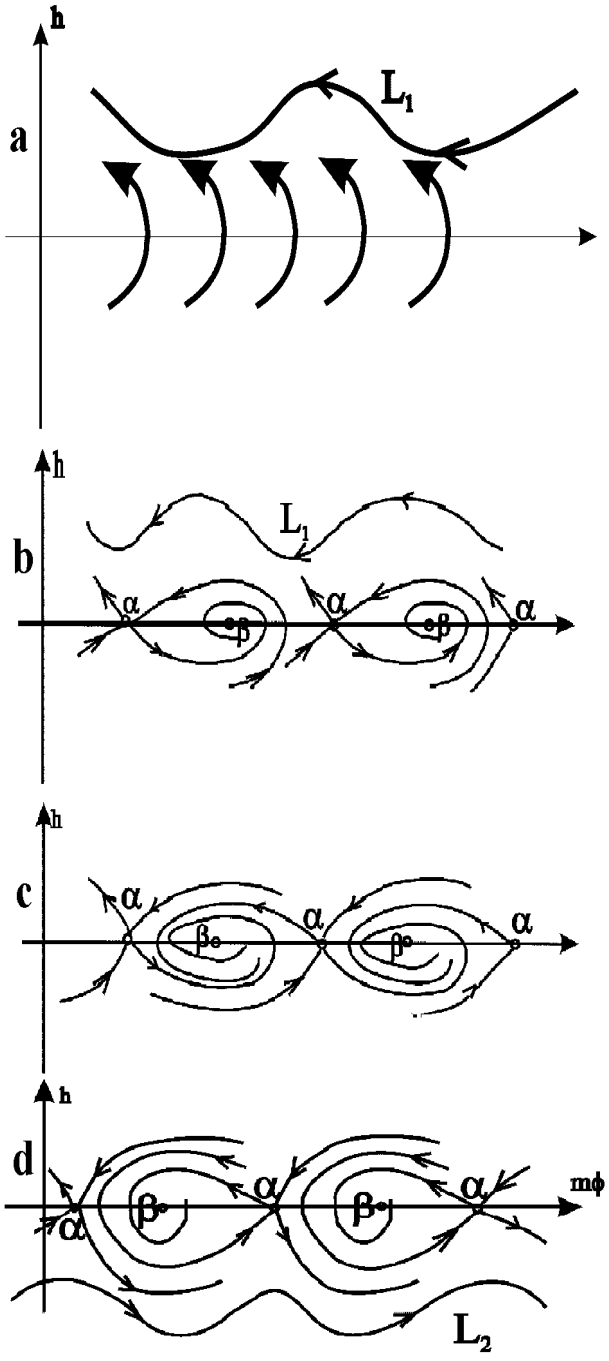

Figure 2.6: The phase portraits of dynamical system.

satisfies the equation α=0. This equation describes the bifurcation curve H (Figure 2.5) on the parameter plane $(\delta_L,\Gamma_t)\in R^2$, which can be written as

$$\Delta_1 = \Delta_1^{(H)}(k);\ \lim_{k\to 1}\Delta_1^{(H)}(k) = \frac{15\delta}{8\pi^4\sqrt{\lambda}}\left[\frac{\Omega\pi}{\lambda}cth(\frac{\Omega\pi}{2\sqrt{\lambda}})+1\right]^{-1}\lim_{k\to 1}k'^2K^2. \tag{2.26}$$

The bifurcation behavior of the system (20) is considered. The bifurcation structure on the parametric plane (δ_L,Γ_t) is qualitatively presented in Figure 2.5. In the regions A and B the motions are qualitatively different, as saddle-node bifurcation line (GZ) separates them. The phase trajectories of the region B are shown qualitatively in Figure 2.6b. Here, the saddle fixed point α, the stable fixed point β and stable periodic motions L_1 take place. As a result of the saddle- node bifurcation *(GZ)* these fixed points are coupled and disappeared. Therefore, there are no fixed points in the region A (Figure 2.5). In this case, only the stable periodic motions L_1 take place (Figure 2.6a). The same bifurcation behavior is observed in $E-F$ region transitions. The saddle-node bifurcation *(RN)* separates these regions.

Heteroclinic orbits of the system (20) are considered. The following values of δ_1 are chosen:

$$\delta_1 = \delta_*(m) + \sqrt{\varepsilon}\Delta; \quad \Delta = O(2.1). \tag{2.27}$$

The equations (2.27) are substituted into (20) and the Hamiltonian of the system (20) is the following:

$$H = \frac{\sqrt{\varepsilon}}{2}\frac{\partial\omega}{\partial I}\bar{h}^2 + \frac{\sqrt{\varepsilon}\Gamma\pi\, J_3}{2m}\cos m\bar{\phi}. \tag{2.28}$$

The dynamical system (2.28) has the following fixed points: centers $(\bar{\phi}_\nu,\bar{h}_\nu) = \left(\frac{2\nu}{m}\pi;0\right)$; ν=0;$\pm$1...; and saddles $(\bar{\phi}_\nu,\bar{h}_\nu) = \left(\frac{2\nu+1}{m}\pi;0\right)$. The heteroclinic orbits joint the saddles fixed points. Taking into account (2.28), the heteroclinic orbits in dissipative dynamical system (20) are calculated by means of the following Melnikov function:

$$\bar{M} = -\frac{\sqrt{\varepsilon}}{2}\frac{\partial\omega}{\partial I}\Delta\pi^3\sqrt{\lambda}J_2\int\limits_{-\infty}^{\infty}\bar{h}dt + \sqrt{\varepsilon}\frac{\partial\omega}{\partial I}\,\chi|_{\Delta=0}\int\limits_{-\infty}^{\infty}\bar{h}^2dt. \tag{2.29}$$

Integration in the equation (2.29) is performed taking into account the Hamiltonian (2.28). Then the heteroclinic bifurcations take place, if the system parameters satisfy the following equation:

$$\Delta = \pm\frac{4\,\chi|_{\Delta=0}}{J_2\sqrt{\lambda}}\sqrt{\frac{2\Gamma J_3}{m\pi^7\left|\frac{\partial\omega}{\partial I}\right|}}. \tag{2.30}$$

The heteroclinic bifurcations sets (ZQ) and (RS) are presented qualitatively in Figure 2.5. Let us consider the bifurcations, when the system passes from the region B to the regions C and D. The periodic motions L_1 are observed in the region B (Figure 2.6b). These periodic motions are connected with the heteroclinic orbit. Note, that this heteroclinic trajectory is observed on the bifurcation curve *(ZQ)*. There are no periodic motions in the region C (Figure 2.6c). The heteroclinic trajectory is observed on the bifurcation curve *(RS)*. Moreover, the periodic motion L_2 is born from this heteroclinic trajectory. These periodic motions take place in the region D (Figure 2.6d).

The system (20) having the homoclinic trajectory was obtained by the averaging method. This method is applied to nonautonomous systems, which is derived from the

system (2.17) using the change of the variables (2.18). At some system parameters, the homoclinic trajectory of the autonomous system (20) corresponds to the separatrix manifolds intersections of saddle periodic motions in nonautonomous equations. The Smale horseshoes arise due to these intersections in phase space. Such phenomenon for the Duffing–Van-der-Pol oscillator is considered in the paper [16]. The intersections of invariant manifolds in the system (2.6) are not considered in this paper.

3 Domains of Chaotic Frictional Vibrations Under the Action of Almost Periodic Excitation

One degree- of- freedom system (Figure 3.1) is considered in this section. The Duffing oscillator under the action of almost periodic force interacts with moving belt. The vibrations of the discrete mass is described by the general coordinate x. It is assumed, that the belt moves with constant velocity v_*, interacting with oscillator due to the dry friction $f(v_R)$, where v_R is relative velocity of rubbing surfaces. The nonlinear spring is described by the restoring force: $R = cx + c_3x^3$. The system vibrations are excited by the following almost periodic force:

$$p(t) = \Gamma_1 \cos\omega_1 t + \Gamma_2 \cos\omega_2 t.$$

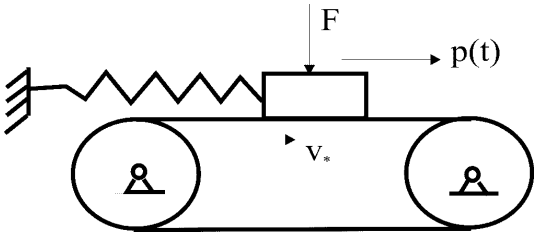

Figure 3.1: The Duffing oscillator interacting with moving belt.

The equation of the system motions has the following form:

$$m\ddot{x} + cx + c_3x^3 = \Gamma_1 \cos\omega_1 t + \Gamma_2 \cos\omega_2 t - f(\dot{x} - v_*); \tag{3.1}$$

$$f(\dot{x} - v_*) = \theta_0 sign(\dot{x} - v_*) - A(\dot{x} - v_*) + B(\dot{x} - v_*)^3. \tag{3.2}$$

We use the next dimensionless variables and parameters:

$$\varepsilon\mu\gamma_2 = \frac{\Gamma_2}{cx_*}; \alpha = \frac{A\omega_0 x_*}{\theta_0}; \beta = \frac{B\omega_0^3 x_*^3}{\theta_0};$$

$$x = x_*\xi(t); \tau = \omega_0 t; \Omega_1 = \frac{\omega_1}{\omega_0}; \Omega_2 = \frac{\omega_2}{\omega_0}; \varepsilon\lambda = \frac{c_3x_*^2}{c}; \varepsilon\mu\tilde{\theta} = \frac{\theta_0}{cx_*}; \varepsilon\gamma_1 = \frac{\Gamma_1}{cx_*}, \tag{3.3}$$

where μ, ε are two independent small parameters:$0 \prec \varepsilon \prec\prec \mu \prec\prec 1$. The mechanical system (3.1) with respect to dimensionless variables and parameters is written in the form:

$$\xi'' + \xi = \varepsilon\left\{-\lambda\xi^3 + \gamma_1 \cos\Omega_1\tau + \mu\left[\gamma_2 \cos\Omega_2\tau - \tilde{\theta}P(\xi' - v_B)\right]\right\}; \tag{3.4}$$

$$P(\xi' - v_B) = sign(\xi' - v_B) - \alpha(\xi' - v_B) + \beta(\xi' - v_B)^3.$$

The second small parameter μ points, that the friction force is essentially smaller than the nonlinear part of the restoring force and the amplitude of the harmonic γ_1 is significantly larger than the amplitude $\mu\,\gamma_2$.

In the future analysis the vibrations are treated for the resonance case:

$$\Omega_1 = 1 + \varepsilon\sigma; \quad \Omega_2 = \Omega_1 + \varepsilon\,\Delta, \tag{3.5}$$

where σ, Δ are two independent detuning parameters. Note, that in the case of the resonance (3.5) the external force is almost periodic. Using the multiple scales method [18], the following system of modulation equations is derived:

$$\begin{aligned} \rho' = \sqrt{\rho}\frac{\gamma_1}{\sqrt{2}}\sin\theta + \mu\Big\{ \rho\,\tilde{\theta}(\alpha - 3\beta v_B^2) - \tilde{\theta}\alpha_1\sqrt{2\rho} - \frac{3}{2}\tilde{\theta}\,\beta\,\rho^2 + \\ + \sqrt{\rho}\frac{\gamma_2}{\sqrt{2}}\sin\theta\cos\Delta T_1 + \sqrt{\rho}\frac{\gamma_2}{\sqrt{2}}\cos\theta\sin\Delta T_1\Big\}; \end{aligned} \tag{3.6}$$

$$\theta' = \sigma - \frac{3\lambda}{4}\rho + \frac{\gamma_1}{2\sqrt{2\rho}}\cos\theta + \mu\frac{\gamma_2}{2\sqrt{2\rho}}(\cos\theta\cos\Delta T_1 - \sin\theta\sin\Delta T_1); \tag{3.7}$$

$$\alpha_1(\rho) = \begin{cases} 0; v_B > \sqrt{2\rho}; \\ \frac{2}{\pi}\sqrt{1 - \frac{v_B^2}{2\rho}}; v_B < \sqrt{2\rho}, \end{cases}$$

where $(\cdot)' = \frac{d(\cdot)}{dT_1}$; $\quad T_1 = \varepsilon\tau$. Note, that the dynamical system (36, 37) has small parameter μ.

The general coordinate ξ of the system (3.4) and the modulation variables (ρ, θ) are connected as

$$\xi = \sqrt{2\rho}\cos(\Omega_1\tau - \theta) + O(\varepsilon). \tag{3.8}$$

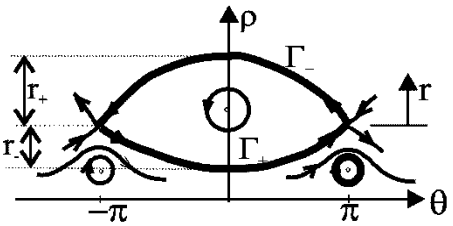

Figure 3.2: The phase portraits of the Hamiltonian system (3.9).

Unperturbed system (36, 37) (μ=0) has the following Hamiltonian:

$$H = -\sqrt{2\rho}\frac{\gamma_1}{2}\cos\theta + \frac{3\lambda}{8}\rho^2 - \sigma\rho. \tag{3.9}$$

The system with Hamiltonian (3.9) has two groups of fixed points (θ_1, ρ_1) and (θ_2, ρ_2), which satisfy the next cubic equation:

$$\sigma - \frac{3\lambda}{4}\rho_{1,2} \pm \frac{\gamma_1}{2\sqrt{2\rho_{1,2}}} = 0; \theta_1 = 0; \theta_2 = \pm\pi. \tag{3.10}$$

These fixed points are shown in Figure 3.2. They are two types of the points: centers and saddles. The saddle fixed points are connected by heteroclinic orbits $\Gamma_-(\rho_-(T_1);\theta_-(T_1))$ and $\Gamma_+(\rho_+(T_1);\theta_+(T_1))$ (Figure 3.2). The trajectories Γ_- and Γ_+ correspond to upper and lower heteroclinic orbit, respectively. From the equation (3.7) at μ=*0,* it is derived:

$$\theta_\pm(\tau) = \arcsin\left(\frac{\sqrt{2}\rho'_\pm}{\gamma_1\sqrt{\rho_\pm}}\right).$$

This equation is substituted into (3.6) assuming that μ=*0.* As a result one has:

$$\rho'^2 = \left(\frac{\gamma_1\sqrt{\rho}}{\sqrt{2}} + \sigma\rho - \frac{3\lambda}{8}\rho^2 + H_s\right)\left(\frac{\gamma_1\sqrt{\rho}}{\sqrt{2}} - \sigma\rho + \frac{3\lambda}{8}\rho^2 - H_s\right). \tag{3.11}$$

The equation (3.11) is solved using the change of the variables

$$\rho(T_1) = \rho_2^{(2.1)} + r(T_1);$$

and the initial conditions

$$\theta_\pm(0) = 0; \rho_\pm(0) = \rho_2^{(2.1)} + \tilde{r}_\pm, \tilde{r}_\pm = 2(k \pm \sqrt{2k\rho_2^{(2.1)}}); k = \frac{4\sigma}{3\lambda} - \rho_2^{(2.1)}.$$

As a result it is derived:

$$\rho_\pm(T_1) = \rho_2^{(2.1)} \pm \frac{2\tilde{r}_-\tilde{r}_+}{(\tilde{r}_+ - \tilde{r}_-)ch(\tilde{a}T_1) \pm (\tilde{r}_+ + \tilde{r}_-)}, \tag{3.12}$$

where $\tilde{a} = \frac{3\lambda}{8}\sqrt{-\tilde{r}_-\tilde{r}_+}$, $\rho_2^{(2.1)}$ is coordinate of the saddle fixed point.

The intersections of the invariant manifolds take place in the perturbed system (36, 37). The theory of such intersections is treated in books [1,2]. The Smale horseshoe, which is the simplest mathematical pattern of chaotic vibrations, appears due to such heteroclinic structure. The Melnikov function [1] is used to determine the region, where the heteroclinic structure exists. The method for these functions calculations is considered in [1]. Here this approach is used to determine the region of heteroclinic orbits existence in the system of modulation equations (36, 37). The heteroclinic Melnikov function of the system (36, 37) has the following form:

$$\begin{aligned}\tilde{M} = \int\limits_{-\infty}^{\infty} \{-\tfrac{\gamma_1\gamma_2}{4}\sin\theta\cos(\Delta t - \Delta t_0 + \theta) + \tfrac{\gamma_2}{\sqrt{2}}\sqrt{\rho}\sin(\Delta t - \Delta t_0 + \theta)\times \\ \times\left(\sigma - \tfrac{3}{4}\lambda\rho + \tfrac{\gamma_1}{2\sqrt{2\rho}}\cos\theta\right)\Big\}\, dt + \int\limits_{-\infty}^{\infty} \mathrm{P}(\rho)\left(\sigma - \tfrac{3}{4}\lambda\rho + \tfrac{\gamma_1}{2\sqrt{2\rho}}\cos\theta\right) dt,\end{aligned} \tag{3.13}$$

where $\mathrm{P}(\rho) = -\tilde{\theta}\alpha_1\sqrt{2\rho} + \rho\tilde{\theta}(\alpha - 3\beta\, v_B^2) - \frac{3}{2}\tilde{\theta}\beta\rho^2$. The integrals (3.13) are determined using the heteroclinic trajectories of the system (36, 37) at μ=*0.* On performing the integration (3.13), the following equations are taken into account:$\rho(T_1) = \rho(-T_1); \theta(T_1) = -\theta(-T_1)$. As a result of the transformations, the Melnikov function is derived in the following form:

$$\begin{aligned}\tilde{M} = \tfrac{\gamma_2}{2}\sin(\Delta t_0)\left\{\int\limits_{-\infty}^{\infty}\left(-\sigma\sqrt{2\rho}\cos\theta\ + \tfrac{3\lambda}{4}\rho\sqrt{2\rho}\cos\theta - \tfrac{\gamma_1}{2}\right)\cos(\Delta t)dt + \right. \\ \left. + \sigma\int\limits_{-\infty}^{\infty}\sqrt{2\rho}\sin\theta\sin(\Delta t)dt - \tfrac{3\lambda}{4}\int\limits_{-\infty}^{\infty}\rho\sqrt{2\rho}\sin\theta\sin(\Delta t)dt\right\} + \\ + \int\limits_{-\infty}^{\infty}\mathrm{P}(\rho)\left(\sigma - \tfrac{3}{4}\lambda\rho + \tfrac{\gamma_1}{2\sqrt{2\rho}}\cos\theta\right)dt.\end{aligned} \tag{3.14}$$

Conclusively, the Melnikov function is written in the form:

$$\tilde{M}_{\pm}(t_0) = \frac{\gamma_2}{2} A_{\pm} \sin(\Delta t_0) + D_{\pm}. \tag{3.15}$$

The parameter $D_{\pm}$ is derived as:

$$D_{\pm} = \mp \left(3\beta\, v_B^2 - \alpha\right) \tilde{\theta} \frac{16}{3\lambda} \left(\sigma\theta_0^{\pm} \mp \frac{9\lambda}{16}\tilde{\rho}\right) + \tilde{\theta}\beta \left\{\frac{14\tilde{\rho}\sigma}{\lambda} \mp \theta_0^{\pm} \left[\left(9\rho_2^{(1)} - \frac{4\sigma}{\lambda}\right) \times \right.\right.$$
$$\left.\left. \times \left(\frac{4\sigma}{\lambda} - 2\rho_2^{(1)}\right) + \frac{7\sigma(\tilde{r}_+\tilde{r}_-)}{\lambda}\right]\right\} + \tilde{\theta}\frac{9\lambda}{16} J_2^{(\pm)} + \tilde{\theta}\left(\frac{9}{8}\lambda\rho_2^{(1)} - \frac{\sigma}{2}\right) J_1^{(\pm)},$$

where $\theta_0^+ = \theta_0; \theta_0^- = \pi - \theta_0; \theta_0 = \arccos\left(\frac{\tilde{r}_+ + \tilde{r}_-}{\tilde{r}_+ - \tilde{r}_-}\right); \tilde{\rho} = \sqrt{-\tilde{r}_+\tilde{r}_-}$.

The parameters $J_2^{(\pm)}$ and $J_1^{(\pm)}$ are not presented here for brevity. The values $A_{\pm}$ are determined as:

$$A_{\pm}(\Delta, \lambda, \gamma_1, \sigma) = \frac{9\lambda^2}{16\gamma_1} K_3^{\pm} - \frac{9\lambda}{8\gamma_1}(2\sigma - \frac{3}{2}\rho_2^{(1)}\lambda) K_2^{\pm} -$$
$$-\frac{1}{2\gamma_1}\left[\frac{9}{4}\gamma_1\lambda\sqrt{2\rho_2^{(1)}} - \sigma(4\sigma - 3\lambda\rho_2^{(1)})\right] K_1^{\pm} - \frac{3\lambda}{2\gamma_1} L_1^{\pm} + \left(\frac{2\sigma}{\gamma_1} - \frac{3\lambda}{2\gamma_1}\rho_2^{(1)}\right) L_0^{\pm}, \tag{3.16}$$

where

$$K_n^{\pm} = \int_{-\infty}^{\infty} r_{\pm}^n(t)\cos(\Delta t)dt; L_n^{\pm} = \int_{-\infty}^{\infty} r_{\pm}^n(t)\dot{r}_{\pm}(t)\sin(\Delta t)dt; n = 1, 2, 3. \tag{3.17}$$

The integrals (3.17) satisfy the following equations:

$$L_0 = -\Delta K_1; K_2 = -\frac{2}{\Delta} L_1. \tag{3.18}$$

Values of the integrals are determined using the residuals. As a result, the f ollowing parameters are calculated:

$$K_1^{\pm} = \mp \frac{16\pi\ sh(\Delta'\theta_0^{\pm})}{3\lambda sh(\Delta'\pi)}; \quad K_2^{\pm} = \frac{16\pi\tilde{\rho}}{3\lambda}\left[\Delta' \frac{ch(\Delta'\theta_0^{\pm})}{sh(\Delta'\pi)} \mp ctg\theta_0 \frac{sh(\Delta'\theta_0^{\pm})}{sh(\Delta'\pi)}\right];$$

$$K_3^{\pm} = \mp \frac{8\pi\tilde{\rho}^2}{3\lambda sh(\Delta'\pi)} \left\{sh(\Delta'\theta_0^{\pm})(1 + 3ctg^2\theta_0 + \Delta'^2) \mp 3\Delta' ctg\theta_0 ch(\Delta'\theta_0^{\pm})\right\};;$$

$$L_0^{\pm} = \pm \frac{16\Delta\pi\ sh(\Delta'\theta_0^{\pm})}{3\lambda sh(\Delta'\pi)}; \quad L_1^{\pm} = -\frac{8\Delta\pi\tilde{\rho}}{3\lambda}\left[\Delta' \frac{ch(\Delta'\theta_0^{\pm})}{sh(\Delta'\pi)} \mp ctg\theta_0 \frac{sh(\Delta'\theta_0^{\pm})}{sh(\Delta'\pi)}\right],$$

where $\Delta' = \frac{8\Delta}{3\tilde{\rho}\lambda}$. Then, finally, the value of $A_{\pm}(\Delta, \lambda, \gamma_1, \sigma)$ has the following form:

$$A_{\pm}(\Delta, \lambda, \gamma_1, \sigma) = \cos ech\left(\frac{8\Delta\pi}{3\tilde{\rho}\lambda}\right)\left\{\mp\left[\frac{8\pi\Delta}{3\lambda\gamma_1}\left(\frac{3}{2}\lambda\tilde{\rho}ctg\theta_0 - 2\left[2\sigma - \frac{3}{2}\lambda\rho_2^{(1)}\right]\right) + \right.\right.$$
$$\frac{2\pi}{3\lambda\gamma_1}\left\{\frac{27}{4}\lambda^2\tilde{\rho}^2 ctg^2\theta_0 - 9\lambda\tilde{\rho}(2\sigma - \frac{3}{2}\rho_2^{(1)}\lambda)ctg\theta_0 - 9\gamma_1\lambda\sqrt{2\rho_2^{(1)}} + \right.$$
$$\left.\left. +8\sigma(2\sigma - \tfrac{3}{2}\rho_2^{(1)}\lambda) + \tfrac{9}{4}\lambda^2\tilde{\rho}^2\right\} + \tfrac{\pi\Delta^2 32}{3\gamma_1\lambda}\right]\ sh(\Delta'\theta_0^{\pm}) +$$
$$\left. + \left[\frac{\Delta^2\pi 32}{3\gamma_1\lambda} + \frac{8\pi\Delta}{\lambda\gamma_1}\ \left\{\frac{3}{2}\tilde{\rho}\lambda\, ctg\theta_0 - 2(2\sigma - \frac{3}{2}\rho_2^{(1)}\lambda)\right\}\right]\ ch(\Delta'\theta_0^{\pm})\right\}. \tag{3.19}$$

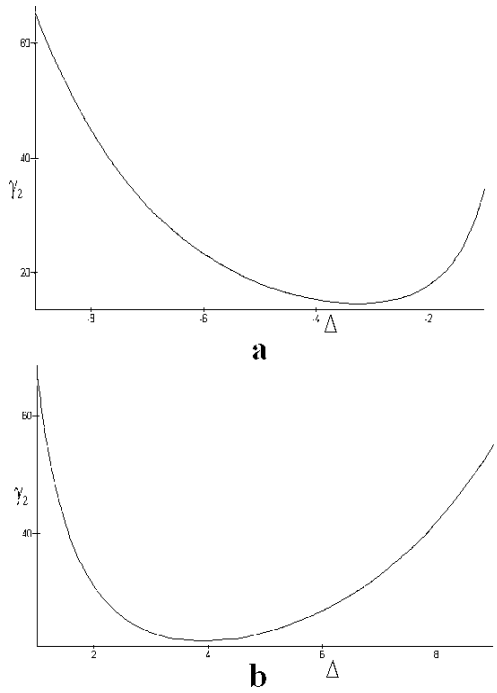

Figure 3.3: The boundaries of the regions of chaotic vibrations.

As shown in the book [1], the intersections of invariant manifolds are described by the simple roots of the equation: $\tilde{M}_{\pm}(t_0) = 0$. The homoclinic structure is observed in the region, where the following inequality is met:

$$\left|D_{\pm}A_{\pm}^{-1}\right| < 0.5\gamma_2^{(\pm)}. \tag{3.20}$$

The region of chaotic vibrations (3.20) is studied numerically. The following parameters of the mechanical system (3.1) are used in the future analysis [19]:

$$m = 0.981kg;\ c = 9.81 \cdot 10^3 \frac{N}{m};\ c_3 = 1.67 \cdot 10^3 \frac{N}{m^3};\ \Gamma_1 = 100N;\ \theta_0 = 4.9N;$$
$$A = 0.2\frac{kg}{s};\ B = 3 \cdot 10^{-6}\frac{kg \cdot s}{m^2}.$$

Then dimensionless parameters (3.3) have the following values:

$$\varepsilon = 0.01; \mu = 0.1; \lambda = 17; \tilde{\theta} = 0.5; \gamma_1 = 1.02; \alpha = 4.08; \beta = 0.61; \sigma = 10; \nu_B = 4.$$

Figure 3.3a, b shows boundaries of the chaotic vibrations regions, $\gamma_2^{(+)}(\Delta)$ and $\gamma_2^{(-)}(\Delta)$, for the above-presented system parameters. The heteroclinic structures of the modulation equations (36, 37) take place above these boundaries.

4 Boundary Values Problem for the HT Construction

4.1 Convergence condition

Let us assume that there are local expansions of solution obtained at small and large values of a parameter c (for example, the parameter is an amplitude value or initial energy of the system). For small values of c the local expansion can be determined as a power series in c, while for large values of c it can be determined as a power series in c^{-1}:

$$y^{(0)} = \alpha_0 + \alpha_1 c + \alpha_2 c^2 + ..., \qquad y^{(\infty)} = \beta_0 + \beta_1 c^{-1} + \beta_2 c^{-2} + ... \tag{4.1}$$

In order to join local expansions (4.1), fractional rational diagonal two-point PA [8] can be used. Let us consider the PA of the form:

$$PA_s = \frac{\sum\limits_{j=o}^{s} a_j\, c^j}{\sum\limits_{j=o}^{s} b_j\, c^j} = \frac{\sum\limits_{j=o}^{s} a_j\, c^{j-s}}{\sum\limits_{j=o}^{s} b_j\, c^{j-s}}, \quad s = 1, 2, , ... \tag{4.2}$$

By comparison of expressions (4.1) and (4.2) and retaining only terms with the order of ^{r} $(-s \le r \le s)$, one obtains a system of $2(s{+}1)$ linear algebraic equations for the determination of coefficients a_j, b_j $(j = 0, \ldots, s)$. Since generally the determinant of the system Δ_s, is not equal to zero, the system has a single trivial exact solution. But we need in PA corresponding to the retaining terms in Eq. (2.1) having non-zero coefficients a_j, b_j. Without loss of generality it can be assumed that b_0 =1. Now, the system of algebraic equations for determination of a_j, b_j becomes overdetermined. All of the unknown coefficients can be determined from (2s+1) equations while the "residual" of this approximate solution can be obtained by substitution of all the coefficients into the remaining equation. Obviously, the residual (or "error") is determined by the value of Δ_s (it can be proved), since the non-zero solution for coefficients and consequently PA will be obtained in the given approximation by c only in the case when Δ_s= 0. Hence the following is a necessary condition for convergence of the succession of PA_s in the form (2.2) at $s \to \infty$ to the fractional rational function which gives us a presentation of the solution for all values of the parameter c [10-12]. Namely,

$$\lim_{s\to\infty} \Delta_s^{(i)} = 0 \;\; (i = 2, 3, ..., n)\,. \tag{4.3}$$

It is possible to generalize the necessary condition for convergence (4.3) to quasi-PA_s which contain both powers of some unknown parameter, and exponential functions [9]. Besides, it is possible to utilize the condition (4.3) for obtaining some unknown parameters which are contained in local expansions [20].

4.2 Potentiality condition and condition at infinity

It is assumed that along the closed HT the dynamical system energy is saved in average. For the single-DOF dynamical system of the form,

$$\ddot{x} + f(x, \dot{x}, t) = 0,$$

Multiplying the last equation by $\dot{x}(t)$ and integrating within limits from $t = 0$ to $t = \pm\infty$, (or from $t = -\infty$ to $t = +\infty$) along the HT one has the following:

$$\oint f(x, \dot{x}, t)\, \dot{x}\, dt = 0. \tag{4.4}$$

Note that such condition is used in many problems of the perturbation theory [18] to construct periodic solutions. In this case the integration is made by the solution period. This condition for periodic solution is called the periodicity one.

Additionally we are going to find the solution $x(t)$ as an analytic function along the HT satisfying the next condition:

$$(x(t), \dot{x}(t)) \underset{t\to\pm\infty}{\longrightarrow} (b_0,\ 0)\,. \tag{4.5}$$

That is we suppose that HT tends to the equilibrium point (saddle point) at infinity.

The convergence condition (4.3), and conditions presented in this subsection, permit to solve uniquely the boundary-value problem for the HT. It is possible to construct both this trajectory and the corresponding solution in time.

5 Non-autonomous Duffing Equation

5.1 Analytical construction of the homoclinic trajectory

One considers in details the construction of HT for the well-known non-autonomous Duffing equation. In general case this equation has a form

$$\ddot{y} + \delta\dot{y} - \beta\, y + \alpha\, y^3 = f\cos\omega\, t, \tag{5.1}$$

A lot of papers are devoted to the investigation of this equation and systems described by it [1, 4-7, 22-24]. Chaotic behavior of solutions can be observed at different choices of elastic characteristics, namely for soft elasticity ($\beta < 0,\ \alpha < 0$) [21], rigid one ($\beta < 0,\ \alpha > 0$) [22], with zero ($k = 0,\ \gamma > 0$) [23] or negative ($\beta > 0,\ \alpha > 0$) [5, 24] linear elasticity.

Here the last variant, namely, $\beta > 0$, $\alpha > 0$, $\delta > 0$, $\delta << 1,\ f << 1$, is considered. In this case the unperturbed system has three equilibrium positions, namely one unstable saddle point $(0, 0)$ and two stable nods $\left(\pm\sqrt{\beta/\alpha}, 0\right)$. To simplify notations let us do the change of variables $y = \lambda x,\ t = \mu\tau$ to make coefficients of x and x^3 equal to -1 and 1, correspondingly. Then equation (2.1) can be rewritten as

$$y'' + \delta\, y' -\ y +\ y^3 = f\cos\omega\, t. \tag{5.2}$$

A problem of effective analytic approximation of HT in non-autonomous system is not solved up to now. Here PA and QRA [8, 9] are used for the HT and the corresponding time solution construction in the case of small dissipation.

To construct the HT in this system we should determine values of the system parameters $\delta,\ \omega,\ f$, corresponding to this trajectory and the coordinates of the shifted saddle point $(b_0, 0)$. The coordinates of the initial point for this trajectory (a_0, a_1) are also required. Thus we have to construct system of four equations to find unknowns. The condition (4.5) at infinity will be used.

Thus, we can consider the next expansion of the solution of equation (5.2) in Taylor series at zero:

$$y\ =\ a_0\ +\ a_1 t\ +\ a_2 t^2\ +\ a_3 t^3\ +\ a_4 t^4\ +\ a_5 t^5\ +\ a_6 t^6 + \ldots, \tag{5.3}$$

where a_0, a_1 are arbitrary constants. After substitution of (5.3) to the equation (t) and equating the coefficients at equal powers of variable t, we get the following expressions

for series coefficients:

$$a_2 = -(a_0^3 - a_0 - f + \delta\, a_1)/2, \quad a_3 = (a_1 - 3a_0^2 a_1 - 2\delta\, a_2)/6,$$
$$a_4 = (2a_2 - f\omega^2 - 6\delta\, a_3 - 6a_1^2 a_0 - 6a_2 a_0^2)/24, \quad \dots$$

Multiplying the equation (5.2) by $y'(t)$ and integrating within limits from $t = 0$ to infinity along the homoclinic trajectory, we have the following:

$$-\frac{b_0^2}{2} + \frac{a_0^2}{2} + \frac{b_0^4}{4} - \frac{a_0^4}{4} - \frac{a_1^2}{2} + \int_0^{\pm\infty} (\delta\, y' - f\ \cos\ \ \omega\ t)\ y'\, dt = 0. \tag{5.4}$$

Let us consider the integral $\int_0^T (\delta\, y' - f\ \cos\ \ \omega\, t)\ y' dt$. After substitution instead of $y(t)$ its Taylor series and integration one obtains:

$$\int_0^T (\delta\, y' - f\ \cos\ \ \omega\, t)\ y' dt = A\, T + B\, T^2 + C\, T^3 + D\, T^4 + E\, T^5 + \cdots\,, \tag{5.5}$$

where

$$A = (\delta\, a_1 - f)a_1,\ B = (2(\delta\, a_1 - f)a_2 + 2\delta\, a_2 a_1)/2,$$
$$C = \big(3(\delta\, a_1 - f)a_3 + 4\delta\, a_2^2 + (f\omega^2/2 + 3\delta\, a_3)a_1\big)/3,$$
$$D = \big(4(\delta\, a_1 - f)a_4 + 4\delta\, a_4 a_1 + 6\delta\, a_2 a_3 + 2(f\omega^2/2 + 3\delta\, a_3)a_2\big)/4, \dots$$

It is desirable to get presentation of the integral at infinity. For this the QPA is used as a form of analytical continuation of the expansion (5.5):

$$A\, T + B\, T^2 + C\, T^3 + \cdots \to PA_3^p = \frac{\alpha_1 T + \alpha_2 T^2 + \alpha_3 T^3}{1 + \beta_1 T + \beta_2 T^2 + \beta_3 T^3}. \tag{5.6}$$

From here one has the following:

$$\alpha_1 = A,$$
$$\alpha_2 = -\frac{-ADC^2 - DA^2E + 2AD^2B + FA^2C - AFB^2 + B^3E - 2B^2DC + BC^3}{AEC - AD^2 - B^2E + 2BDC - C^3},$$
$$\alpha_3 = (-A^2E^2 + 2AEC^2 + 2AEBD - 2ACD^2 - 2ACBF + DFA^2$$
$$-2CB^2E + 3BDC^2 - D^2B^2 + FB^3 - C^4)/(AEC - AD^2 - B^2E + 2BDC - C^3),$$
$$\beta_2 = -\frac{AE^2 - EC^2 - EBD + CD^2 + CBF - DFA}{AEC - AD^2 - B^2E + 2BDC - C^3},$$
$$\beta_3 = \frac{-BDF + BE^2 - 2DCE + C^2F + D^3}{AEC - AD^2 - B^2E + 2BDC - C^3}.$$

Passing on to infinity in the fractional presentation (5.6), we can rewrite the equation (5.4) as:

$$-\frac{b_0^2}{2} + \frac{a_0^2}{2} + \frac{b_0^4}{4} - \frac{a_0^4}{4} - \frac{a_1^2}{2} + \frac{\alpha_3}{\beta_3} = 0. \tag{5.7}$$

Additional equation could be obtained from the convergence condition for the PA (5.6):

$$\begin{aligned}&-2D^2BF+2DBE^2-3D^2CE+2DC^2F+D^4-AE^3+E^2C^2-2ECBF+\\&2EDFA-F^2AC+F^2B^2+GAEC-GAD^2-GB^2E+2GBDC-GC^3=0.\end{aligned}\tag{5.8}$$

In similar way we can construct the analytical continuation of the solution at infinity by means of quasi-rational approximation. This QPA is chosen in the form similar to the solution of autonomous Duffing equation (separatrix solution), namely:

$$y=a_0\ +\ a_1t\ +\ a_2t^2\ +\ a_3t^3\ +\ldots\to e^{-t}\frac{\alpha_0+\alpha_1e^t+\alpha_2e^{2t}+\alpha_3e^{3t}}{1+\beta_2e^{2t}}.\tag{5.9}$$

It follows from (5.9) that

$$b_0=\frac{\alpha_3}{\beta_2},\tag{5.10}$$

where coefficients α_i, β_j in (5.9) can be found as it is described below.

Final equation being the convergence condition for the approximation (5.9) is

$$\begin{aligned}&24a_5a_3+2a_5a_1+12a_5a_2-24a_4^2-4a_1a_4-\frac{4}{15}a_1a_2-\frac{7}{10}a_1a_3-\\&-\frac{1}{10}a_1^2-8a_2a_4+\frac{5}{6}a_2^2+4a_2a_3+6a_3^2-12a_4a_3=0.\end{aligned}\tag{5.11}$$

The system of algebraic equations (5.7), (5.8), (5.10) and (5.11) determines the unknown values a_0, a_1, b_0 and $f=f(\delta)$ while ω is fixed. They can be obtained from the essentially nonlinear system by means of the Newton method. Several examples of obtained phase trajectories are presented in Figure 5.1 and Figure 5.2. Figure 5.1 shows trajectories constructed by Runge–Kutta procedure with initial points obtained from the system. Here two sets of parameters are chosen, namely:

a) $\delta=0.001$, $a_0=1.21508$, $a_1=0.621819$, $b_0=0.00058$, $f=0.00087$; $\omega=1$;

b) $\delta=0.01$, $a_0=1.21609$, $a_1=0.621943$, $b_0=0.0058$, $f=0.00878$, $\omega=1$.

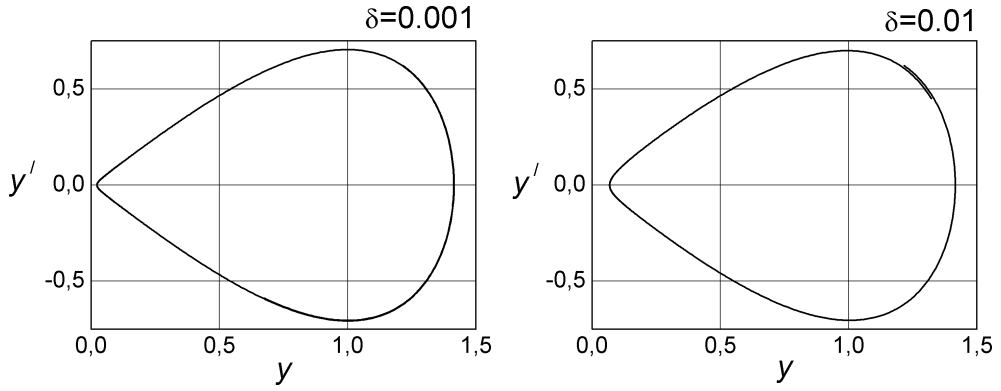

Figure 5.1: Trajectories constructed by Runge–Kutta procedure with initial points obtained from the system (5.7), (5.8), (5.10) and (5.11).

Figure 5.2 gives comparison of trajectories constructed with the same initial point obtained from the system but in different ways, namely by means of Runge–Kutta method

(solid line) and by the QPA (5.9) (dash line). Values of parameters are taken as for the previous figure.

Figure 5.3 and Figure 5.4 present parameter dependences corresponding to the HT creation, i.e. chaos onset. The solid lines show curves obtained by the proposed approach, but dash lines show the same curves obtained by the Melnikov method. Numerical investigation of chaos onset in the system under consideration shows that our curve is more exact.

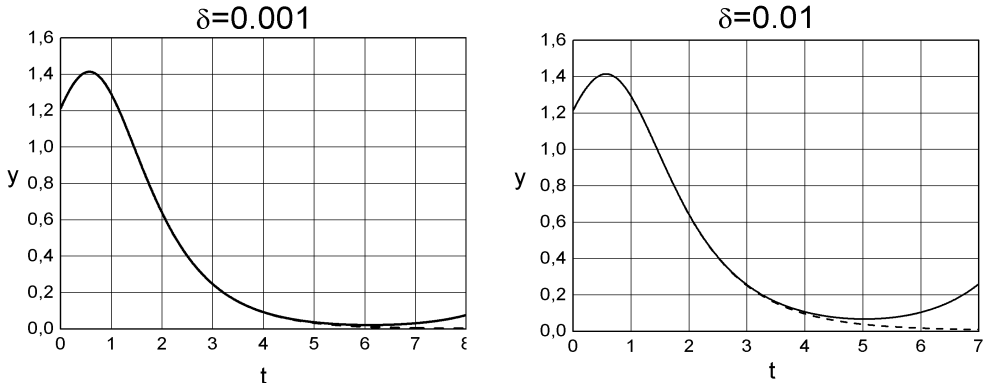

Figure 5.2: Comparison of the trajectories constructed with the obtained initial point by Runge–Kutta method (solid line) and by means of quasi-rational approximation (dash line).

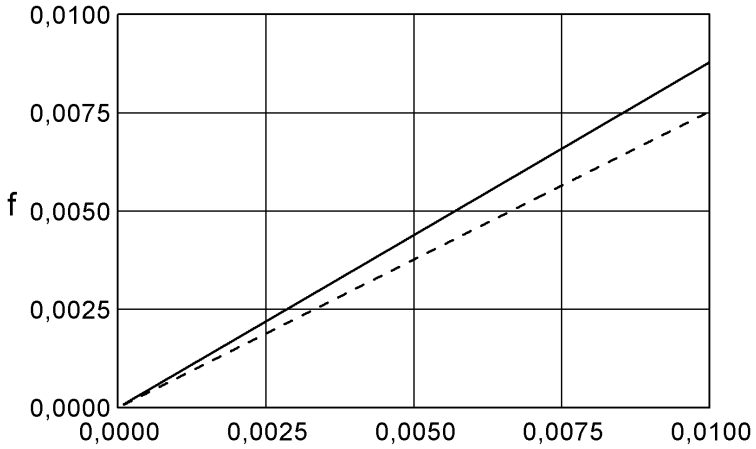

Figure 5.3: Dependence between the amplitude of external force and dissipation coefficient for $\omega = 1$.

Introduction of the phase φ permits to choose the point $(a_0, 0)$ as the HT initial point instead of such point (a_0, a_1) as was made earlier. The corresponding HT construction is not presented here, and it can be found in [25].

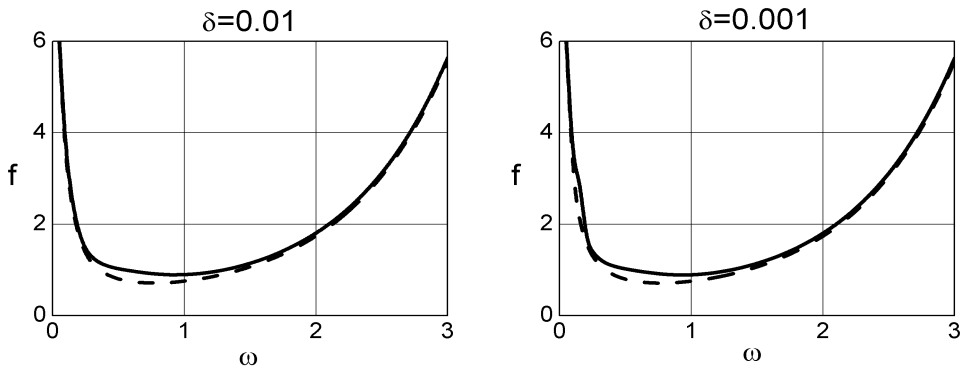

Figure 5.4: Dependence (ω, f) corresponding to HT appearance.

5.2 Comparison of analytical construction and numerical simulation

The obtained analytical results can be compared with numerical simulation. The numerical construction of the manifolds was fulfilled to find the moment of the separatrix branches touching, which corresponds to the chaos onset. The method of Latte [26] was used for this. The main idea of this approach is to consider quadratic approximation of manifolds:

$$y - y_0 = \alpha\,(x - x_0) = \alpha_1^{\pm}\,(x - x_0) + \frac{\alpha_2^{\pm}}{2}\,(x - x_0)^2 + O\left(|x - x_0|^3\right),$$

where "+" corresponds to unstable manifold but "–" corresponds to stable one. Here (x_0, y_0) is saddle point in phase space. Figure 5.5 and Figure 5.6 present the fulfilled investigation and demonstrate the accuracy of the obtained above analytic results (values of parameters corresponding to manifold touching are the same as obtained above analytically).

Value of the force amplitude corresponding to a point of the HT formation obtained by the analytical approach is equal to 0.004465 for some fixed values of ω and δ. The same result is observed in Figure 5.5.

Figure 5.6 presents phase portraits when $\omega = 2$, $\delta = 0.001$ and $\delta = 0.01$. Corresponding analytic results are $f = 0.0018$ and $f = 0.018$.

6 Construction of the HT in Different Dynamical Systems

6.1 The Van der Pol–Duffing equation

One considers the model which describes, in particular, the panel flatter in the supersonic air flow [25]:

$$\ddot{x} + \delta\left(\alpha - \beta x^2\right)\dot{x} - x + x^3 = 0, \tag{6.1}$$

where α, $\beta > 0$, δ is the small parameter $(0 < \delta << 1)$.

To construct the HT, the procedure presented in the previous Section, is used here. At first, local expansions near the unstable equilibrium point are selected. These expansions, corresponding to stable and unstable branches, can be obtained by using the small

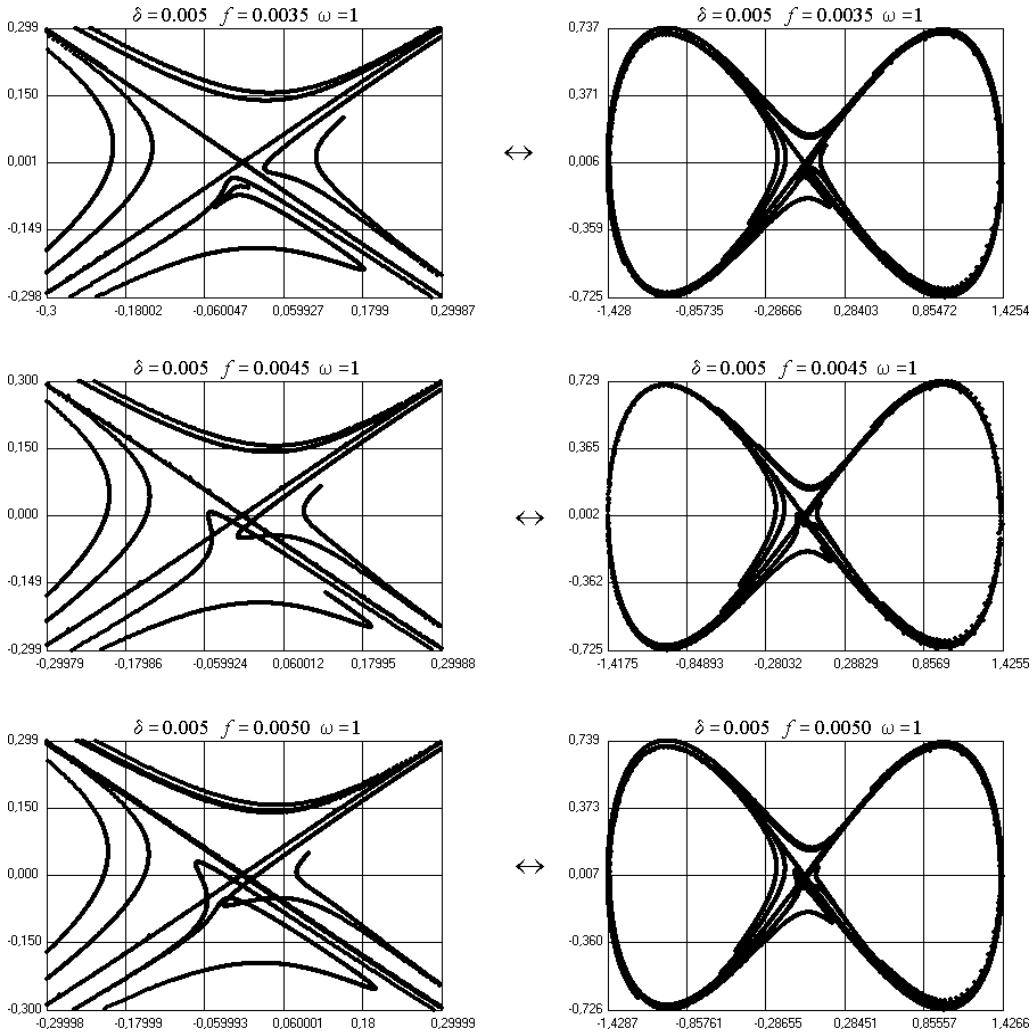

Figure 5.5: Phase portraits for Duffing equation when $\delta = 0.005,\ \omega = 1$.

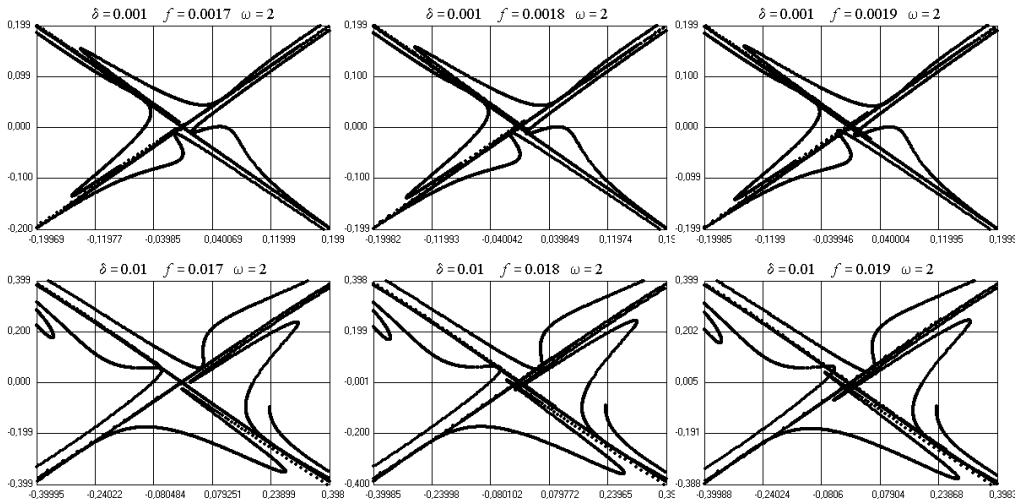

Figure 5.6: Phase portraits of Duffing system in the vicinity of the saddle point.

parameter method:

$$x = c_0 e^{k_1 t} - c_0^3 \frac{1 - k_1 \delta\beta}{9k_1^2 + 3\delta\alpha k_1 - 1} e^{3k_1 t} + \ldots, \quad t \to +\infty; \tag{6.2}$$

$$x = c_1 e^{k_2 t} - c_1^3 \frac{1 - k_2 \delta\beta}{9k_2^2 + 3\delta\alpha k_2 - 1} e^{3k_2 t} + \ldots, \quad t \to -\infty, \tag{6.3}$$

here $k_1 = \dfrac{-\delta\alpha - \sqrt{\delta^2\alpha^2 + 4}}{2}$, $k_2 = \dfrac{-\delta\alpha + \sqrt{\delta^2\alpha^2 + 4}}{2}$ are roots of the characteristic equation $k^2 + \delta\alpha\ k - 1 = 0$, and c_0, c_1 are arbitrary constants. One writes too the Taylor series for a solution $x(t)$ at point $t = 0$:

$$x = a_0 + a_2 t^2 + a_3 t^3 + a_4 t^4 + a_5 t^5 + a_6 t^6 + \ldots, \tag{6.4}$$

where a_0 is an arbitrary constant, $a_2 = \dfrac{a_0 - a_0^3}{2}$, $a_3 = -\dfrac{\delta\left(-\alpha + \beta a_0^2\right)\ a_0\left(a_0^2 - 1\right)}{6}, \ldots$

Thus, to construct the HT it is necessary to find values of the three pointed out arbitrary constants, c_0, c_1, a_0. Respectively, three algebraic equations to obtain these constants must be constructed.

Multiplying the equation (6.2) by $\dot{x}(t)$ and integrating within limits from $t = 0$ to infinity along the homoclinic trajectory, we have the following:

$$\frac{a_0^2}{2} - \frac{a_0^4}{4} + \delta \int_0^{\pm\infty} \left(\alpha - \beta x^2\right)\ \dot{x}^2\ dt = 0.$$

Using in this integral the local expansion (6.4), and rebuilding the obtained expression to the Pade approximation, we can write the following:

$$\int_0^t \left(\alpha - \beta x^2\right)\ \dot{x}^2\ dt = At^3 + Bt^4 + Ct^5 + \ldots = \frac{\alpha_3 t^3 + \alpha_4 t^4}{1 + \beta_1 t + \beta_2 t^2 + \beta_3 t^3 + \beta_4 t^4},$$

One has in the limit at $t \to \pm\infty$:

$$\frac{a_0^2}{2} - \frac{a_0^4}{4} + \delta\frac{\alpha_4}{\beta_4} = 0. \tag{6.5}$$

Taking into account the local expansions at infinity (6.2) (6.3), it is possible to match these expansions with the expansion (6.4) by using the QPA of the form

$$P_{+\infty} = e^{k_1 t}\frac{\alpha_0 + \alpha_2 e^{2k_1 t} + \alpha_4 e^{4k_1 t}}{1 + \beta_2 e^{2k_1 t} + \beta_4 e^{4k_1 t}}, \quad P_{-\infty} = e^{k_2 t}\frac{\alpha_0 + \alpha_2 e^{2k_2 t} + \alpha_4 e^{4k_2 t}}{1 + \beta_2 e^{2k_2 t} + \beta_4 e^{4k_2 t}}, \tag{6.6}$$

where coefficients of approximations $P_{+\infty},\ P_{-\infty}$ are calculated by comparing them with the expansions (6.2), (6.4) (6.3), (6.4), respectively.

So, there are two solution presentations for positive and for negative values of the variable t, and we can obtain two additional equations which are the convergence conditions (4.3) for approximations $P_{+\infty},\ P_{-\infty}$. These equations together with the condition of potentiality (6.5) form a system of nonlinear algebraic equations to determine unknown constants presented in local expansions.

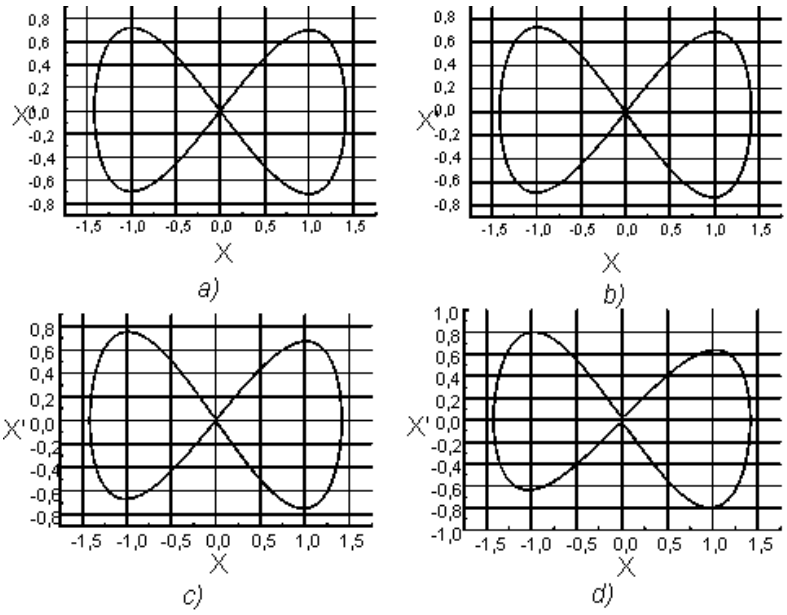

Figure 6.1:

In Figure 6.1 the examples of HT determined by the Runge–Kutta method are shown for different values of the parameter δ, namely: a) $\delta = 0.05$; b) $\delta = 0.1$; c) $\delta = 0.2$; d) $\delta = 0.4$, where the initial values determined from the algebraic equations are used. Figure 6.2 presents a comparison of the HT, obtained by the Runge–Kutta method (line a) and the QPA (6.6) (i.e. $P_{-\infty}$(line b) and $P_{+\infty}$(line c)) for $\delta = 0.01$.

6.2 Equation of a parametrically excited damped pendulum

Let us use the same technique to investigate the behavior of pendulum with periodically excited point of pendulum suspension [27]. This system is governed by the following

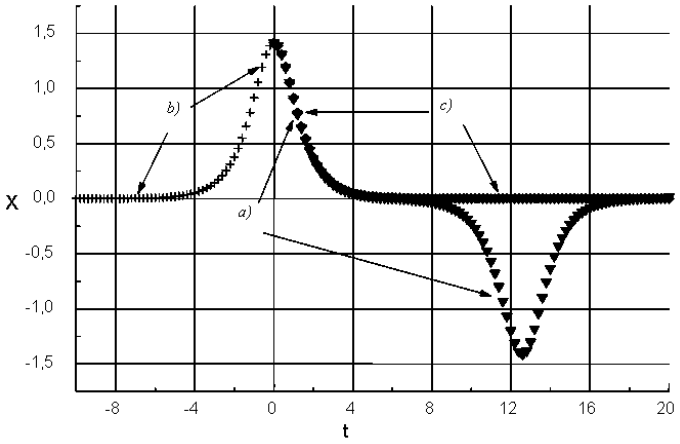

Figure 6.2:

equation:

$$x'' + \delta\, x' + (1 + f\cos\omega\, t)\, \sin x = 0, \tag{6.7}$$

where x is an angle of deviation from the vertical line. We rewrite this equation (6.7) in the form

$$y'' + \delta\, y' - (1 + f\cos\omega\, t)\, \sin y = 0, \tag{6.8}$$

after change $y = x + \pi$. This system possesses infinite number of saddle points $(2\pi\, n, 0)$ $(n \in Z)$, therefore we will consider heteroclinic trajectory construction as criterion of chaos onset. We make the same assumptions as for Duffing equation and obtain the following:

$$\int_0^\infty (y'' + \delta\, y' - (1 + f\cos\omega\, t)\, \sin y)\, y' dt =$$

$$= -\frac{a_1^2}{2} + \cos(b_0) - \cos(a_0) + \int_0^\infty (\delta\, y' - f\cos\omega\, t\, \sin y)\, y' dt = 0.$$

$$\int_0^\infty (\delta\, y' - f\cos\omega\, t\, \sin y)\, y' dt = \left(A\, t + B\, t^2 + C\, t^3 + D\, t^4 + E\, t^5 + \cdots\right)\Big|_0^\infty,$$

where $A = a_1\,(\delta a_1 - f\sin a_0)$, $B = a_1\,(2\delta a_2 - f a_1\cos a_0)/2 + a_2\,(\delta a_1 - f\sin a_0), \ldots$

For analytic continuation we use the quasi-rational approximation:

$$A\, t + B\, t^2 + C\, t^3 + D\, t^4 + E\, t^5 + \cdots \to \frac{\alpha_1 t + \alpha_2 t^2}{1 + \beta_1 t + \beta_2 t^2}, \tag{6.9}$$

where $\alpha_1 = A$, α_2=(–2ABC+$DA_2 + B_3$)/(B_2–AC), β_1=(DA–BC)/(B_2–AC), β_2=(BD–C_2)/(AC–B_2).

Thus we have:

$$-\frac{a_1^2}{2} + \cos\,(b_0) - \cos\,(a_0) + \frac{\alpha_2}{\beta_2} = 0. \tag{6.10}$$

To simplify the problem we accept $b_0 = 0$. Additionally we continue the Taylor series of solution in quasi-rational approximation:

$$y = a_0 \ + \ a_1 t \ + \ a_2 t^2 \ + \ a_3 t^3 \ + \ldots \to e^{-t} \frac{\alpha_0 + \alpha_1 e^t + \alpha_2 e^{2t}}{1 + \beta_2 e^{2t}}. \tag{6.11}$$

The following two algebraic equations are obtained from existence condition for (76) and (78):

$$2CBD - C^3 - D^2 A + EAC - EB^2 = 0, \tag{6.12}$$

$$\begin{gathered} 6a_1a_2 - 72a_2a_3 + 42a_1^2 - 30a_1a_3 + 3a_0a_1 - 18a_0a_3 + 36a_4a_0 + \\ +72a_4a_1 + 72a_4a_2 - 72a_3^2 - 3a_2a_0 - 6a_2^2 = 0. \end{gathered} \tag{6.13}$$

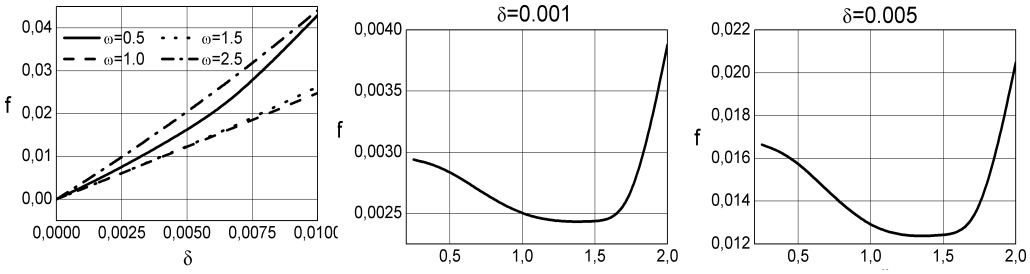

Figure 6.3: Dependences between parameters corresponding to HT creation.

Equations (6.10), (79), (80) form the system of nonlinear algebraic equations to determine parameters of (6.8) and a_0, a_1 while ω is fixed. Figure 6.3 demonstrates the dependences between parameters obtained from constructed system.

At values of force amplitude f less then 0.2, the instability domain is observed only in vicinity of heteroclinic trajectory but at rising of f the domain enlarges as well.

Figure 6.4 demonstrates the results of manifolds construction for the system (6.8) for $\delta = 0.001$ and $\omega = 1$. Figure 6.5 presents the same construction for $\delta = 0.001$ and $\omega = 2$.

Analytic results obtained above by proposed approach are $f = 0.00243$ ($\omega = 1$) and $f = 0.0038$ ($\omega = 2$). So, comparing the obtained analytical results with the phase portraits we can observe a good accuracy of the analytical results and efficiency of the proposed approach.

Similar equations with parametric periodic excitation can be obtained in a problem of the elastic oscillations absorption by using the snap-through truss as absorber. It was shown that the snap-through truss can be used for effective absorption of longitudinal oscillations of some elastic solid [28]. In this case a big part of the energy of elastic oscillations is transferred to the truss, which has a capacity to jump. But it was shown too [29] that the chaotic behavior, which is not appropriate for this absorption, can appear in this system.

7 The One-degree-of-freedom Weakly Forced Oscillator with Nonlinear Dissipation Forces

Mechanical system with a small periodic external excitation, nonlinear dissipation forces and the Duffing type stiffness is governed by the following second order differential equa-

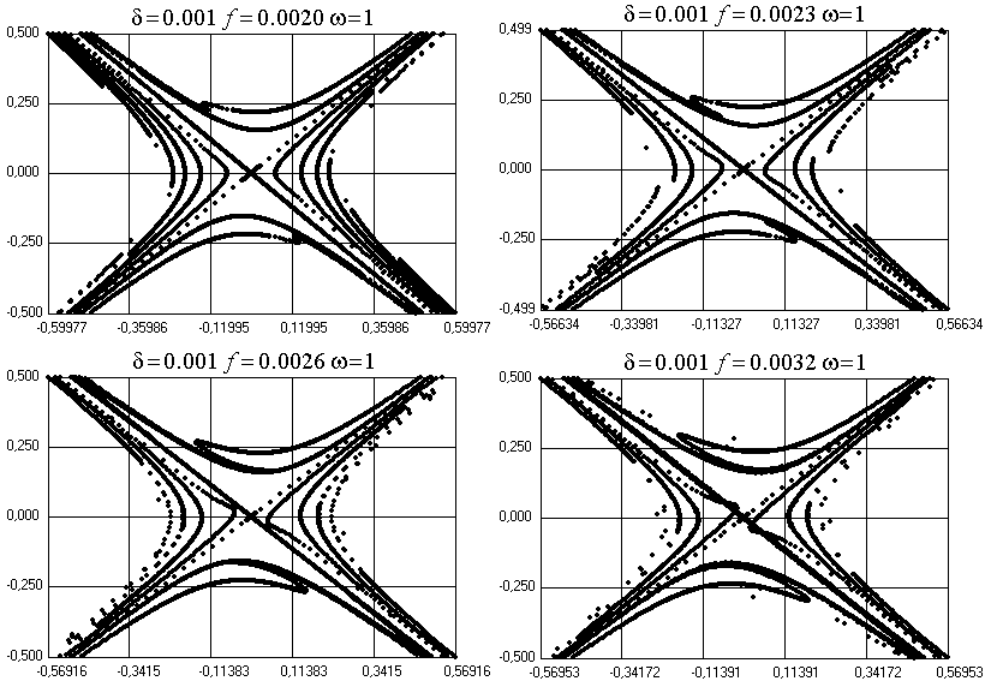

Figure 6.4: Phase portrait of (6.8) in the vicinity of saddle point $(0, 0)$ for $\omega = 1$.

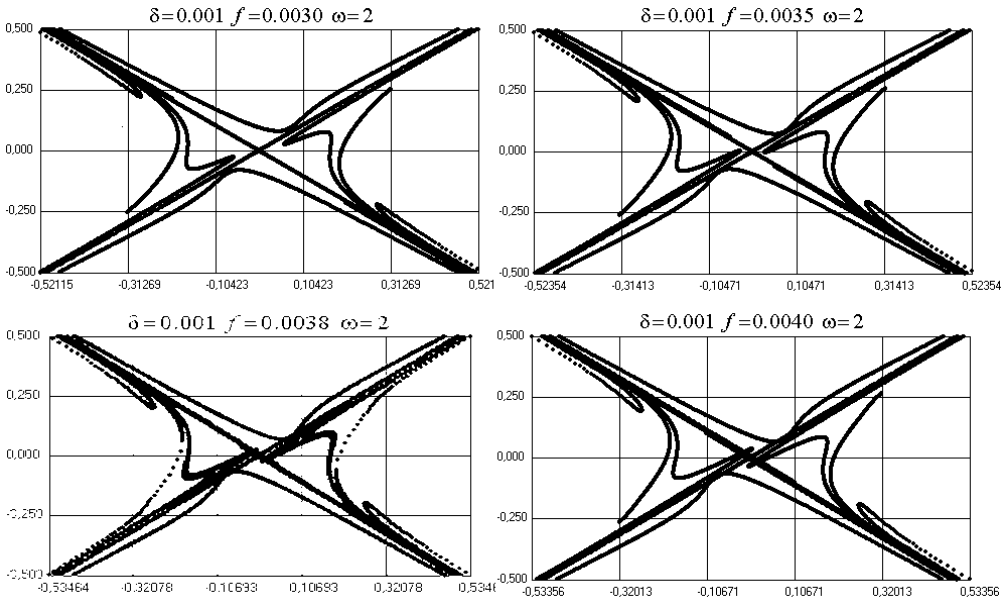

Figure 6.5: Phase portrait of (2.15) in the vicinity of saddle point $(0, 0)$ for $\omega = 2$.

tion:

$$y'' - y + y^3 = f\cos(\omega t + \varphi) - \theta(y' - \nu^*), \tag{7.1}$$

where $\theta(y' - \nu^*) = T_0 sign(y' - \nu^*) - \alpha(y' - \nu^*) + \beta(y' - \nu^*)^3$ is the nonlinear dissipation characteristic.

To construct a homoclinic trajectory we need to know the initial point $(a_0, 0)$, the phase ϕ corresponding to a moment t= 0, and the relation of the system parameters ω, $f$and θ corresponding to HT appearing. Thus we should construct the algebraic system to determine the unknown values.

Let us make some assumption like for the previous systems. One assumes that $(y, y') \underset{t\to\pm\infty}{\longrightarrow} (0,\ 0)$. We will construct the analytical approximation for the sought solution. First, we can consider the Taylor expansion at zero of the solution $y(t)$:

$$y\ =\ a_0\ +\ a_2t^2\ +\ a_3t^3\ +\ a_4t^4\ +\ a_5t^5\ +\ a_6t^6 + \ldots, \tag{7.2}$$

where a_0 is an arbitrary constant, and $a_j = a_j(a_0, \varphi, f, T_0, \alpha, \beta)$ $\left(j = \overline{2, \infty}\right)$

Then multiplying the equation (7.1) by $y'(t)$ and integrating within the limits from $t = 0$ to $t = +\infty$ and from $t = 0$ to $t = -\infty$, one has the following equations where several integrals are calculated along the separatrix zero approximation (for $\theta = 0,\ f\ =\ 0$), $y_0 = \sqrt{2}/ch(t)$:

$$\begin{aligned}\tfrac{a_0^2}{2} - \tfrac{a_0^4}{4} - \left(\alpha\nu^* - \beta\nu^{*3} - T_0\right) a_0 - \tfrac{2\alpha}{3} + \tfrac{8\beta}{35} + \tfrac{4\sqrt{2}\beta\nu^*}{5} + 2\beta\nu^{*2} + \\ + f\sin\varphi \int\limits_0^{+\infty} \sin\,\omega\ t\ y_0'\ dt - f\cos\varphi \int\limits_0^{+\infty} \cos\,\omega\ t\ y_0'\ dt = 0;\end{aligned} \tag{7.3}$$

$$\begin{aligned}\tfrac{a_0^2}{2} - \tfrac{a_0^4}{4} - \left(\alpha\nu^* - \beta\nu^{*3}\right) a_0 + \tfrac{2\alpha}{3} - \tfrac{8\beta}{35} + \tfrac{4\sqrt{2}\beta\nu^*}{5} - 2\beta\nu^{*2} - f\sin\varphi \int\limits_0^{+\infty} \sin\omega\, t\ y_0'\ dt - \\ - f\cos\ \varphi \int\limits_0^{+\infty} \cos\omega\, t\ y_0'\ dt - T_0 \int\limits_{-\infty}^{0} sign\ (y_0' - \nu^*)\ y_0'\ dt = 0.\end{aligned} \tag{7.4}$$

Here

$$\int\limits_0^{+\infty} \sin\omega\ t\, y_0' dt = \int\limits_{-\infty}^{0} \sin\omega\ t\, y_0' dt = -\frac{\omega\sqrt{2}\pi}{2} \cdot \frac{1}{ch\frac{\omega\pi}{2}};$$

$$\int\limits_0^{+\infty} \cos\omega\ t\, y_0' dt = -\int\limits_{-\infty}^{0} \cos\omega\ t\, y_0' dt = -\sqrt{2} + \omega\sqrt{2}\left(-\frac{\pi}{2} th\frac{\omega\pi}{2} + 4\omega\sum_{k=0}^{\infty} \frac{1}{\omega^2 + (1+4k)^2}\right).$$

The integral $\int\limits_{-\infty}^{0} sign\ (y_0' - \nu^*)\ y_0'\ dt$ is evaluated as a function of the parameter ν^* computationally.

For the continuation of the local expansion at infinitum we rebuild it to QPA:

$$y = a_0\ +\ a_2t^2\ +\ a_3t^3\ +\ a_4t^4\ +\ a_5t^5\ + \ldots \to e^{-t}\frac{\alpha_0 + \alpha_1 e^t + \alpha_2 e^{2t}}{1 + \beta_1 e^t + \beta_2 e^{2t}}. \tag{7.5}$$

So, the additional equation may be obtained by means of the convergence equation (4.3) for the QPA (7.5).

$$\begin{aligned}&72a_5a_1a_3+72a_5a_2a_1+12a_5a_1a_0-144a_4a_2a_3-72a_4a_1a_3-\\&-60a_4a_2a_1-72a_5a_3a_0-72a_4a_2^2+72a_2a_3^2+72a_5a_2^2+\\&+30a_5a_1^2+30a_3a_2^2+72a_3^3+3/5a_1a_1a_3-12a_0a_4a_2+\\&+72a_4^2a_0-\frac{1}{10}a_0a_1^2+\frac{1}{2}a_0a_2^2-6a_4a_1^2-\frac{11}{10}a_2a_1^2-\\&-\frac{9}{10}a_1^2a_3+\frac{9}{10}a_1a_2^2+\frac{1}{3}a_1^3+6a_2^3+72a_4^2a_1=0.\end{aligned}\tag{7.6}$$

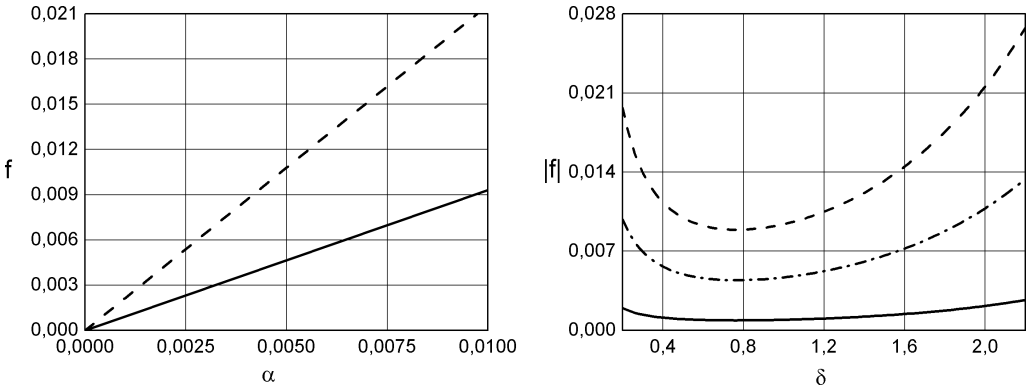

Figure 7.1: Boundaries of the chaotic behavior regions in planes ω, f and δ, f, for ν^*=0.5, $\delta = 0.001$ (solid line), $\delta = 0.005$ ("point-dash" line), $\delta = 0.01$ (dash line).

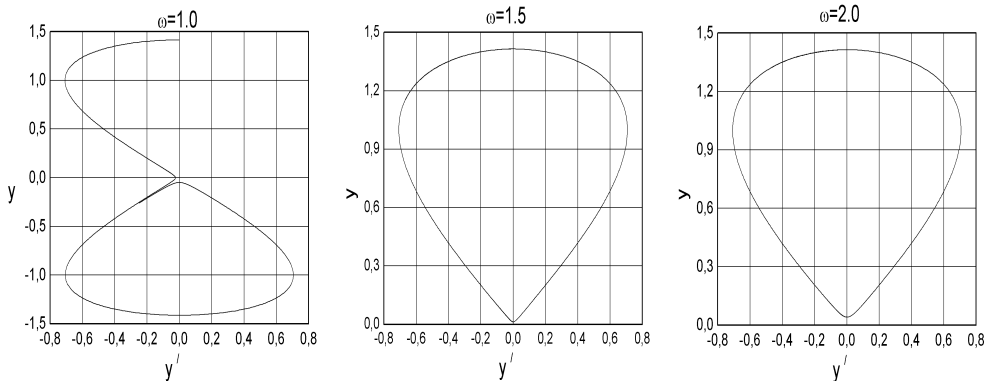

Figure 7.2: Haotic behavior boundaries in parameter spaces and the homoclinic trajectories in phasespace while ν^*=0.5, $T_0 = \alpha = \beta$=0.001.

Nonlinear algebraic equations (7.3), (7.4) and (7.6) form the system which allows to determine unknown parameters a_0, φ and the relation $f = f(\omega)$ while the dissipation parameters T_0, α, β are fixed.

Figure 7.1 shows the dependences between the parameters of the system corresponding to HT and the one obtained by the method proposed here.

Also the example of homoclinic trajectory and comparison of the trajectory evaluated by Runge-Kutta method (when it is used the initial values, obtained from the obtained above algebraic equations) and by means of QPA (7.5) are presented in Figure 7.2.

8 Concluding Remarks

The methodologies presented in this work is sufficiently general to be applicable to other types of non-linear dynamical systems. The subharmonic Melnikov–Morozov theory is utilized to describe a sequence of the saddle-node bifurcations in the process of transition to the chaotic behavior in some mechanical systems. An appearance of heteroclinic structures in mechanical systems under the almost-periodic excitation, is described too by using the Melnikov functions. The multiple-scale method is used here successfully. Other approach of detection of the chaotic behavior is a construction of homo- or heteroclinic trajectories (HT) by using the Pade- and quasi-Pade approximants. It seems more exact that the generally used Melnikov function approach. The presented approach realizes the analytical continuation of the local expansions connected with these HT, to infinity. The necessary condition of convergence of the PA or QPA, as well additional conditions at infinity permit to solve corresponding boundary-value problem for the closed HT. Checking of numerical calculations of the HT with initial amplitudes values obtained by using the analytical approach, shows an acceptable precision of the proposed analytical procedure.

References

[1] Guckenheimer, J. and Holmes, P. *Nonlinear oscillations, dynamical systems and bifurcations of vector fields*. Springer-Verlag, New York, 1993.

[2] Wiggins, S. *Introduction to applied nonlinear dynamical systems and chaos*. Springer-Verlag, New York, 1990.

[3] Bourland, F.J. and Haberman, R. Separatrix crossing: time-invariant potentials with dissipation. *SIAM J. Appl. Math.* 50 (6) (1990) 1716–1744.

[4] Melnikov, V. K. On the stability of the centre for time periodic perturbations. *Trans. Moscow Math. Soc.* 12 (1963) 1–57.

[5] Holmes, P. A nonlinear oscillator with a strange attractor. *Philosophical Transactions of The Royal Society of London, A. Mathematical and Phisical Sciences* **292** (1394) (1979) 419–448.

[6] Moon, F. C. *Chaotic vibrations*. Wiley, New York, 1987.

[7] Sanders, J. A. Melnikov's method and averaging. *Celestial Mech.* **28** (1982) 171–81.

[8] Baker, G. A. and Graves-Morris, P. *Pade' approximants*. Addison-Wesley, London, 1981.

[9] Martin, P. and Baker, G. A. Two-point quasifractional approximant in physics, truncation error. *J. Math. Phys.* **32** (1991) 1470.

[10] Manevich, L. I., Mikhlin, Yu. V. and Pilipchuk, V. N. *The method of normal oscillation for essentially nonlinear systems*. Nauka, Moscow, 1989. (in Russian)

[11] Mikhlin, Yu. V. Matching of local expansions in the theory of nonlinear vibrations. *J. Sound and Vibration* **182** (1995) 577–588.

[12] Vakakis, A. F., Manevich, L. I., Mikhlin, Yu. V., Pilipchuk, V. N. and Zevin, A. A. *Normal modes and localization in nonlinear systems*. Wiley, New York, 1996.

[13] Bolotin, V.V. *The dynamic stability of elastic systems*. Holden-Day, San Francisco, 1964.

[14] Saito, H. and Koizumi, N. Parametric vibrations of a horizontal beam with a concentrated mass at one end. *Int. J. Mech. Sci.* **24** (1982) 755–761.

[15] Abramowitz, M. and Stegun, I.A. *Handbook of mathematical functions*. Dover, New York, 1965.

[16] Greenspan, B. and Holmes, P. Repeated resonance and homoclinic bifurcation in a periodically forced family of oscillators. *SIAM Journal of Math. Anal.* **15** (1984) 69–97.

[17] Morozov, A. D. Approach to a complete qualitative study of Duffing's equation. *USSR J. Comp. Math. and Math.Phys.* **3** (1973) 1134–1152.

[18] Nayfeh, A. H. *Perturbation methods*. Wiley, New York, 1973.

[19] Kononenko, V. *Vibrating Systems with Limited Power Supply*, Illife, London, 1969.

[20] Mikhlin, Yu. V. and Manucharyan, G. V. Construction of homoclinic and heteroclinic trajectories in mechanical systems with several equilibrium positions. *Chaos, Solitons and Fractals.* **16** (2003) 299–309.

[21] Dowell, E. H., Katz, A.L. A Basic explanation of Homoclinic Intersection in Twin-Well Duffing Oscillator. *Fields Institute Communications.* **9** (1996) 65–92.

[22] Virgin, L.N. Approximate criterion for capsize based on deterministic dynamics. *Dynamics and Stability of Systems* **4** (1) (1989) 55–70.

[23] Beirsdorfer, P., Wersinger, J.M. and Treve, Y. Topology of the invariant manifolds of period-doubling attractors for some forced nonlinear oscillators. *Phys. Lett. Ser. A.* **96** (6) (1983) 269–272.

[24] Moon, F.C. Experiments on chaotic motions of a forced nonlinear oscillator: strange attractors. *Journal of Applied Mechanics* **47** (1980) 638–644.

[25] Manucharyan, G.V. and Mikhlin, Yu.V. The construction of homo- and heteroclinic orbits in non-linear systems. *Journal of Applied Mathematics and Mechanics* **69** (2005) 39–48. (in Russian)

[26] Latte's, S. Sur les equations fonctionnelles qui de'finissent une courbe ou une surface invariante par une transformation. *Annali di Matematica* **13** (3) (1906) 1–137.

[27] Leven, R. W. and Koch, B. P. Chaotic behavior of a parametrically excited damped pendulum. *Phys Lett* **86A** (2) (1981) 71–74.

[28] Avramov, K. V. and Mikhlin, Yu. V. Snap-through truss as a vibration absorber. *Journal of Vibration and Control* **10**, 2004, 291–308.

[29] Mikhlin, Yu.V. and Manucharyan, G.V. Determination of the Chaos Onset in Mechanical Systems with Several Equilibrium Positions. *Meccanica* **41** (2006) 253–267.